



# UNIVERSITY OF TWENTE.

Faculty of Engineering Technology,  
Civil Engineering and Management

## Approximating river bed level at river bifurcations if data is scarce

Gerard van Leeuwe  
M.Sc. Thesis  
December 2018

---

**Supervisors:**

Prof. dr. S.J.M.H Hulscher  
Dr. R.M.J. Schielen  
Dr. ir. M.F.M. Yossef  
Ir. J.S. de Jong

Civil Engineering and Management  
Faculty of Engineering Technology,  
River and Coastal Engineering  
University of Twente  
P.O. Box 217  
7500 AE Enschede  
The Netherlands

---

**Deltares**

Enabling Delta Life





# Preface

After a long search for an interesting and challenging thesis subject, I found this assignment of Deltares about river bifurcations. The combination of programming and research did really appeal to me. The fact that one of the results of the thesis a tool, that actually would be used in the future, attracted me too. After working a lot with MATLAB during my bachelor's thesis, programming with Python was a new challenge.

First of all I would like thank my supervisors at Deltares: Jurjen the Jong and Mohamed Yossef. They have helped me greatly with pointing my research in the right direction and keeping in mind the greater picture of the research . Also it was a pleasure to perform this thesis study at Deltares. The working environment and ethics there had a very positive impact on my work.

I would also like to thank Ralph Schielen and Suzanne Hulscher for their supervision from the University of Twente. Especially in the beginning they helped me greatly with getting the project started.

Without the data provided by Maarten Kleinhans, this study would not have been possible. Therefore, I want to thank Maarten for his generous and prompt sharing of the data.

A great thanks to my parents and siblings, especially to my mother who has helped me a lot by proofreading my thesis. At last I would like to thank my girlfriend, Janneke van der Meer, for fully supporting me from the other side of the world.



# Summary

Zervakis (2015) has developed a physics based model that approximates bed level in single river branches, based on parameters like: river slope, discharge, river curvature and river width. This physics based model is developed to support the interpolation of measured data. Fusing results from interpolation and the physics based model reduces the necessary amount of measured data to get bed level approximation with certain accuracy. This thesis study has focussed on extending the rapid assessment tool in such a way that the bed level at river bifurcations can be approximated. Two main goals set: Firstly, describe a bifurcation quantitatively and assessing which parameters are affecting the bed level around a bifurcation. Secondly, assess the performance of interpolation methods that describe the bed level around a bifurcation. The main research question of this thesis is: *What is a method to approximate the bed level of an alluvial river bifurcation if data are scarce and how well does this method perform?*

Kleinhans et al. (2008) used a Delft3D model in their study to the effect of river curvature on the stability of a river bifurcation. The data of that study is used to analyse the effect of four parameters on the transition zone. The effect of: river width, river curvature, the difference in water depth between the start and end of the transition zone and, the discharge distribution on the length of the transition zone and the length and size of bars or pools that occur in the transition zone have been analysed.

Relationships between the upstream transition zone length and both the upstream river width and the upstream river curvature have been identified. The other parameters do not affect the upstream transition zone length. The river width is identified as an indicator for the downstream transition zone length. Due to the set-up of the used model, it could not be established whether the upstream or downstream river width is has a stronger relationship with the downstream river length. The size of the bars and pools is difficult to predict based on the analysed parameters. Only between the river curvature and bars and pools size, a relationship is identified. It is suspected that this relationship is specific for the situations of the scenarios. The length of the bars and pools upstream and downstream is related to the length of the respectively upstream or downstream transition zone length.

These relationships are implemented in the extended rapid assessment tool. Four types of interpolation are implemented: single step without transition zone, linear interpolation, Gaussian error function interpolation and linear interpolation which includes bars and pools.

The accuracy of the extended rapid assessment tool depends on the accuracy of the physics based model. The error in the upstream or downstream zones propagates to the

error in the computed bed level in the transition zone. This causes the interpolation methods to perform all about equally well. The error in all cases is similar to the error outside the transition zone. When the measured data as basis for the interpolation, the difference in performance of the interpolation methods becomes significant. The single step method performs worst, the linear interpolation performs well in most study cases. In one study cases the addition of bars and pool to the linear interpolation increases the accuracy.

The identified relationships between the various parameters and the transition zone length or bars and pools can possibly depend on the used water depth data. Parameters like the discharge, river slope, and downstream river width have not been varied but may have an effect on the transition zone and the bars and pools.





# Contents

<b>Preface</b>	<b>iii</b>
<b>Summary</b>	<b>v</b>
<b>Notation</b>	<b>xiii</b>
<b>1 Introduction</b>	<b>1</b>
1.1 Motivation . . . . .	1
1.2 Research questions . . . . .	2
1.3 Thesis outline . . . . .	2
<b>2 Related work</b>	<b>5</b>
2.1 Rapid assessment tool . . . . .	5
2.1.1 Physics based model . . . . .	5
2.1.2 Interpolation . . . . .	7
2.2 Relevant literature . . . . .	8
2.2.1 Water depth up and downstream of a bifurcation . . . . .	8
2.2.2 Transition zone length . . . . .	9
2.2.3 Effect of sedimentation and erosion zones . . . . .	11
2.3 Conclusions . . . . .	11
<b>3 Methodology</b>	<b>13</b>
3.1 Bifurcation analysis method . . . . .	13
3.1.1 Modelled data . . . . .	14
3.1.2 Schematization method . . . . .	15
3.1.3 Analysed parameters . . . . .	16
3.1.4 Cross-sectional profiles . . . . .	17
3.2 Implementation . . . . .	18
3.3 Evaluation method . . . . .	18
3.3.1 Transition zone . . . . .	19
3.3.2 Visual evaluation . . . . .	19
3.3.3 RMSE . . . . .	19
<b>4 Bifurcation analysis</b>	<b>21</b>
4.1 Modelled data . . . . .	21

4.1.1	Validation schematization method . . . . .	22
4.2	Analysis of the effect of parameters on the transition zone . . . . .	24
4.2.1	The effect of difference in water depth on the transition zone . . . . .	24
4.2.2	The effect of discharge distribution on the transition zone . . . . .	24
4.2.3	The effect of river width on the transition zone . . . . .	26
4.2.4	The effect of upstream curvature on the transition zone . . . . .	26
4.2.5	The effect of difference in water depth on bars and pools . . . . .	28
4.2.6	The effect of river width on bars and pools . . . . .	28
4.2.7	The effect of upstream river curvature on bars and pools . . . . .	30
4.2.8	The effect of the transition zone length on bars and pools . . . . .	30
4.2.9	The effect of bar or pool length on the size of bar or pool . . . . .	32
4.3	Cross-sectional profiles . . . . .	32
4.4	Conclusions . . . . .	32
<b>5</b>	<b>Implementation</b>	<b>35</b>
5.1	Grid construction . . . . .	35
5.2	Bed level approximation . . . . .	38
5.3	Interpolation methods . . . . .	39
5.3.1	Single step method . . . . .	39
5.3.2	Linear interpolation . . . . .	39
5.3.3	Gaussian error function interpolation . . . . .	39
5.3.4	Linear interpolation with bars and pools . . . . .	40
5.4	Cross-sectional profiles . . . . .	41
<b>6</b>	<b>Results</b>	<b>43</b>
6.1	Study cases . . . . .	43
6.1.1	Pannerdensche Kop . . . . .	44
6.1.2	IJssel Kop . . . . .	47
6.1.3	Danube - Bala . . . . .	51
6.2	Sensitivity analysis . . . . .	55
6.3	Summary . . . . .	57
<b>7</b>	<b>Discussion</b>	<b>59</b>
7.1	Bifurcation analysis . . . . .	59
7.2	Performance of the extended rapid assessment tool . . . . .	60
7.2.1	Physics based model . . . . .	61
7.2.2	Interpolation methods . . . . .	61
7.3	Study cases . . . . .	62
7.3.1	Pannerdensche Kop . . . . .	62
7.3.2	IJssel Kop . . . . .	62
7.3.3	Danube - Bala bifurcation . . . . .	63
7.3.4	Other suitable cases . . . . .	63

---

<b>8</b>	<b>Conclusions, limitations and recommendations</b>	<b>65</b>
8.1	Conclusions . . . . .	65
8.2	Limitations and recommendations . . . . .	67
	<b>Bibliography</b>	<b>69</b>
	<b>Appendices</b>	
<b>A</b>	<b>Scenarios in Kleinhans et al. (2008)</b>	<b>71</b>
<b>B</b>	<b>Method to create a grid around bifurcations</b>	<b>73</b>
B.1	Finding bifurcation point . . . . .	73
B.2	Preparation . . . . .	73
B.3	Moving vertices . . . . .	73
<b>C</b>	<b>Groynes analysis</b>	<b>75</b>
<b>D</b>	<b>Study case results</b>	<b>77</b>
D.1	Pannerdensche Kop . . . . .	77
D.2	IJssel Kop . . . . .	80
D.3	Danube - Bala bifurcation . . . . .	82



# Notation

$a$ : Calibration coefficient	[-]
$A$ : Coefficient weighing the influence of helical flow	[-]
$C$ : Chézy coefficient	$[m^{1/2}/s]$
$D_{50}$ : Mean grain size diameter	$[m]$
$E$ : Calibration coefficient	[?]
$g$ : Gravitational acceleration	$[m/s^2]$
$h$ : Water depth	$[m]$
$h_C$ : Equilibrium water depth	$[m]$
$i$ : Slope	[-]
$n$ : Mannings coefficient	$[s/m^{1/3}]$
$Q$ : Discharge	$[m^3/s]$
$R$ : Hydraulic radius	$[m]$
$R_C$ : Radius of curvature	$[m]$
TZ : Transition zone	$[m]$
$u$ : flow velocity	$[m/s]$
$v$ : transverse flow velocity	$[m/s]$
$W$ : River width	$[m]$
$\gamma$ : curvature	[-]
$\delta$ : Relative density	$[kg/m^3]$
$\theta$ : Shields parameter	[-]
$\kappa$ : von Karman constant	[-]



# Introduction

Measuring water depth in rivers is costly and time consuming work. In the Netherlands the rivers are closely monitored by Rijkswaterstaat, in order to let ship traffic pass undisturbed. Rijkswaterstaat uses ships with multi-beam systems to measure the water depth in all Dutch waters (Rijkswaterstaat, 2018a). In many countries there is less ship traffic on rivers and much less budget for basic monitoring of the bed level of their rivers. For many situations, knowledge of a river's water depth is important. Knowing the water depth of a river makes it possible to do hydrodynamic analyses. Currently, measurements of cross-sections of the river are used to interpolate and obtain a map of the bed level in a river. By only measuring the bed level at cross-sections with certain intervals between them, the costs and effort may be largely reduced, compared to measuring the whole river. However, this will lead to a map that is less accurate compared to detailed measurements of the whole river. Zervakis (2015) has developed a rapid assessment tool for bed level predictions for Deltares. This tool has been developed to improve the spatial interpolation of water depth measurements in a river branch by combining it with a physics based model. The physics based model computes a cross-sectional profile for a river based on several parameters like discharge, slope and river width. That study found that combining the interpolated data and the basis map will give a more accurate map of the bed level in a river in those cases where data are scarce.

## 1.1 Motivation

The rapid assessment tool developed by Zerkavis can only be applied to single river branches. Most rivers, however, have one or more bifurcations along the way. At these points, the rapid assessment tool cannot be used yet. At the same time, these parts of a river are of importance in many aspects. At a river bifurcation, the discharge downstream is very different from the discharge upstream. The width of a river upstream is often not equal to the sum of the widths of the downstream branches. This and other parameters that change at river bifurcations can lead to different water depths in upstream versus downstream branches.

Generally, the bed level near a bifurcation is not very well characterised. The distribution of discharge and sediment has been the subject of many studies already but these have focused mostly on the morphological stability of a bifurcation. The present study will analyse

the parameters that determine the shape of the bed level at a bifurcation and in which zone the bifurcation influences the bed level.

This knowledge will subsequently be used to extend the rapid assessment tool, in such a way that the river bed level at river bifurcations can also be approximated. As a result, the extended rapid assessment tool will be generally applicable; whole river systems can be assessed by the tool.

## 1.2 Research questions

The main research question for this study will be:

*What is a method to approximate the bed level of an alluvial river bifurcation if data is scarce and how well does this method perform?*

To answer this question four sub-questions have been formulated.

1. *How does the bed level at a bifurcation look?*
2. *Which physical or empirical relationships describe the bed level at bifurcations?*
3. *How can these relationships be implemented in a model?*
4. *How well does the extended tool perform at approximating the bed level at a river bifurcation*

## 1.3 Thesis outline

This report consists of two parts. The first part is focused on the analysis of the bed level around a river bifurcation, the second part aims to implement the found relationships in the extended rapid assessment tool. The chapters are organized as follows:

- ▶ Chapter. 2 covers the literature related to this thesis study described. The tool as developed by Zervakis (2015) is described here as well.
- ▶ Chapter. 3 describes the methodology used in this thesis study. The methods used to analyse the bed level around bifurcations are described. Also, the methods for evaluating the performance of the extended rapid assessment tool are shown here.
- ▶ Chapter. 4 presents the analysis of bifurcations. The effect of various parameters on the transition zone length and bed level have been analysed.
- ▶ Chapter. 5 gives a description of the implementation of the physics based model. The relationships found in the previous chapter are implemented here. Four interpolation methods are used to approximate the bed level in the transition zone.

- 
- ▶ Chapter. 6 presents the results of the application of the tool on three study cases. The characteristics of the measured bed level of the study cases will be compared with the characteristics of the modelled bed level.
  - ▶ Chapter. 7 elaborates on the results and applicability of the extended rapid assessment tool
  - ▶ Chapter. 8 presents the conclusions and recommendations and limitations that follow from this study.



# Related work

In this chapter the relevant literature for this thesis study will be discussed. First, the thesis study of Zervakis (2015) will be summarised here, as this study formed the basis of the present study. Secondly, literature about three aspects of bifurcations will be evaluated. The first aspect is the water depth in the branches up- and downstream of the bifurcation. The second aspect is the river zone upstream of the bifurcation. Here, especially the transition of a single bed to two beds has been investigated. Finally, the effect of sedimentation zones and erosion zones on the bed level around a bifurcation has been investigated.

## 2.1 Rapid assessment tool

Zervakis (2015) has developed a "rapid assessment tool" that models the bed level of an alluvial river. This tool uses a combination of interpolation of available river bed level data and a physics based model to obtain an estimation of river bed level.

First, the general idea behind the tool and its applicability will be explained a bit more. The tool has been created to reconstruct river topography when data are scarce. This is done by combining the results of a physics-based model and spatial interpolation of the available data. Normally, the measured data is used to interpolate and approximate the bed level in a river. The combination of a physics based model and interpolated bed level data gives a higher accuracy of the bed level than only using interpolation of measured data.

This tool has specifically been developed to be applied to meandering alluvial rivers which are mildly curved and have a fairly constant width. To be able to use the interpolation part of the rapid assessment tool, it is required that some data regarding the depth profile of the river is available. Currently, ships sail in a zig-zag trajectory a long a river and measure the water depth or cross-sections of rivers are measured. The rapid assessment tool can use this data for interpolation.

### 2.1.1 Physics based model

The rapid assessment tool uses a simplified physics-based model to compute the bed level of a river. The equilibrium water depth for a river branch is computed based on the Chézy

equation (Eq. 2.2). Due to the curvature in the river a helical flow occurs. This results in a transverse bed slope and an asymmetrical cross-sectional profile where the outer bend will be deeper than the inner bend. Only rivers with mild curvature ratio are taken into account; rivers where the radius of a bend is lower than ten times the river width. Three types of banks can be used in the rapid assessment tool: no banks, linear slope and, Sigmoid slope. An example of a cross-section computed by this method is shown in Figure 2.1, here the sigmoid banks are used. Eq. 2.1 is used to calculate the bed profile. The equation computes the transverse slope of the river bed. The bed level away from the centre of the river is based on the distance to the centre line, the bed level at the centre line and the transverse slope. Eq. 2.3 and 2.5 and the curvature of the river determine the transverse slope of the bed level.

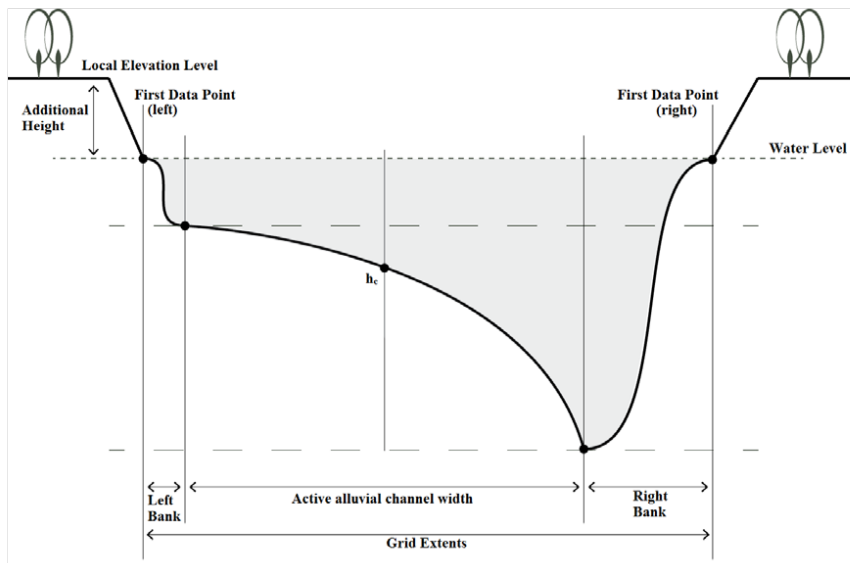


**Figure 2.1:** Physics based bathymetry model cross-section (Zervakis, 2015)

$$h(n) = h_C e^{Af(\theta)n/R_C} \quad (2.1)$$

where:

- $h$  = water depth along  $n$  [m]
- $h_C$  = Equilibrium water depth at centre line. [m]
- $A$  = coefficient weighing the influence of the helical flow
- $f(\kappa)$  = weighing function [-]
- $n$  = coordinate orthogonal to the streamline [m]
- $R_C$  = radius of curvature [m]
- $n$  = distance away from centre line [m]

$$h_C = \left( \frac{Q}{WC\sqrt{i}} \right)^{\frac{2}{3}} \quad (2.2)$$

where:

$Q$  = Discharge [ $m^3/s$ ]

$W$  = River width [ $m$ ]

$C$  = Chézy coefficient [ $m^{1/2}/s$ ]

$i$  = slope [-]

Further defined:

$$A = \frac{2a}{\kappa^2} \left( 1 - \frac{\sqrt{g}}{\kappa C} \right) \quad (2.3)$$

and

$$f(\theta) = \frac{0.85}{E} \sqrt{\theta} \quad (2.4)$$

where:

$a$  = calibration coefficient [-]

$\kappa$  = von Karman constant ( $\approx 0.44$ )

$g$  = gravitational acceleration [ $m/s^2$ ]

$\theta$  = shields parameter [-]

$E$  = calibration coefficient [-]

The last two parameters are:

$$\theta = \frac{u^2 + v^2}{C^2 \delta D_{50}} \quad (2.5)$$

and

$$E = 0.0944 \left( \frac{h}{D_{50}} \right)^{0.3} \quad (2.6)$$

where:

$u, v$  = velocity in stream wise and transverse directions [ $m/s$ ].

$D_{50}$  = mean grain size diameter [ $m$ ]

$\delta = \frac{\rho_s - \rho_w}{\rho_w}$  relative density ( $\rho_s, \rho_w$  sediment and water densities [ $kg/m^3$ ])

### 2.1.2 Interpolation

Four different types of interpolation have been looked into by Zerkavis: Linear, nearest neighbour, Inverse Distance Weighting and Elliptical Inverse Distance Weighting. These interpolation methods are not of interest for this present study and will not be further elaborated on. Eq. 2.7 is used to combine the results from the physics based model and the interpolation. The model weight determines whether the final results are more based on the physics based model or rather on the measured and interpolated data.

$$F_{(s,n)} = w_{(s,n)}PM_{(s,n)} + (1 - w_{(s,n)})I_{(s,n)} \quad (2.7)$$

where:

- $F_{(s,n)}$  = Fusion result at (s,n)
- $PM_{(s,n)}$  = Physics based model result at (s,n)
- $I_{(s,n)}$  = Interpolation of samples result at (s,n)
- $w_{(s,n)}$  = Model weight at (s,n)

Zerkavis concludes that the combination of a physical model and water-flow direction based interpolation gives a better estimation of the river bed level than only interpolation can do when data is scarce.

## 2.2 Relevant literature

This section will discuss the relevant literature in three subsections. In each of these subsections the literature with relation to one aspect of the bifurcation will be elaborated on.

### 2.2.1 Water depth up and downstream of a bifurcation

Wang et al. (1995) was one of the first studies to investigate a 1D model for morphodynamics that included a way to model bifurcations. They developed a nodal point relationship. This relationship was dependent on an exponent  $k$ , which could not be derived mathematically but had to be determined empirically. The model of Wang et al. (1995) was not very suitable for predictions of the evolution of a real bifurcation according to Pittaluga et al. (2003). The use of the  $k$  parameter, which has no relationship to any local conditions and therefore cannot be computed, proved to be the main problem. To overcome this, the nodal point conditions are reformulated by Pittaluga et al. (2003). A quasi two-dimensional scheme was introduced. This scheme is shown in Figure 2.2. Miori et al. (2006) has extended this model further by taking the eroding of banks into account. All three papers conclude their study with findings about the stability of a river bifurcation. The stability is not of interest for the present study.

Both Wang et al. (1995), Pittaluga et al. (2003) and (Miori et al., 2006) use a version of the Chézy formula to calculate the discharge in all three river branches of the bifurcation. When rewritten this equation can be used to calculate the depth based on, among others, the discharge and river width. Wang et al. (1995) uses Eq.2.8, Pittaluga et al. (2003) uses Eq. 2.9 and Miori et al. (2006) uses Eq. 2.10. These equations are almost equal but the Eq. 2.9 and 2.10 have the gravity acceleration in their equation which causes a mismatch in the units.

$$Q = W * C * h^{3/2} * i^{1/2} \quad (2.8)$$

$$Q = W * C * h^{3/2} * (gi)^{1/2} \quad (2.9)$$

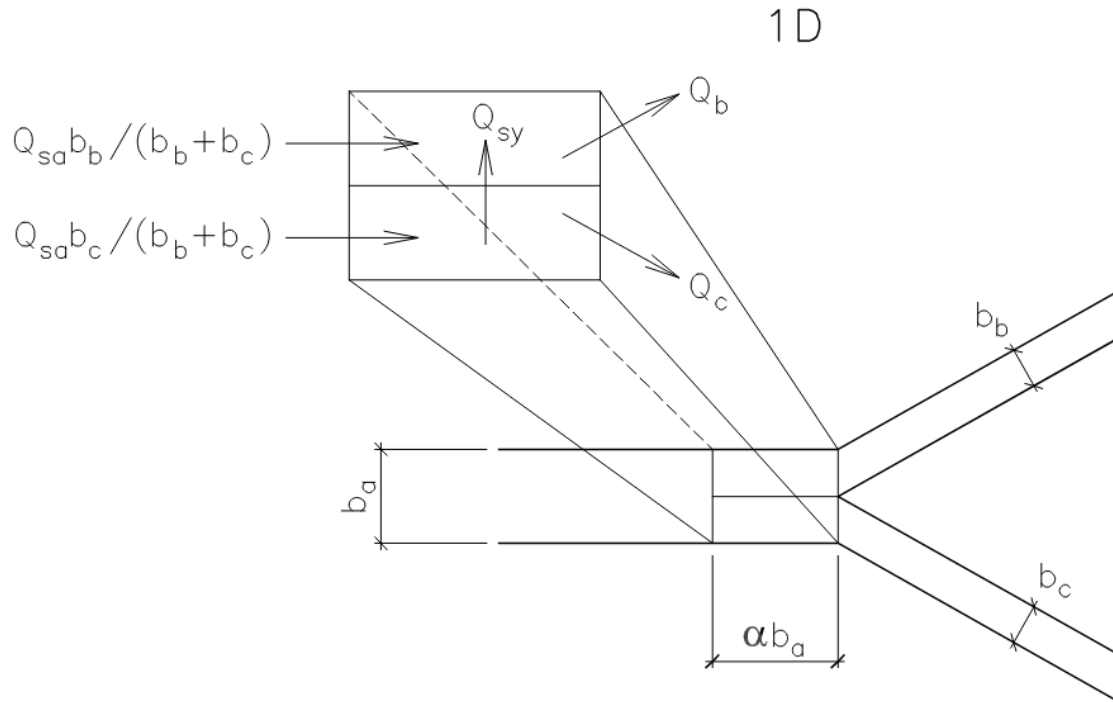


**Figure 2.2:** Quasi 2D scheme for a river bifurcation (Pittaluga et al., 2003)

$$Q = W * C * h * (gRi)^{1/2} \quad (2.10)$$

where:

$R$  = hydraulic radius [m]

$h$  = water depth [m]

### 2.2.2 Transition zone length

According to Pittaluga et al. (2003) the effect of the bifurcation is only noticeable in a short region upstream. The length of this region is assumed to be a factor  $\alpha$  times the width of channel a ( $b_a$ ) and is described as  $\alpha b_a$ . It is assumed to be  $\alpha = 2 - 3$

To estimate the order of magnitude of  $\alpha$  a series of experiments have been carried out. In these experiments the topography of the bed near the bifurcation has been measured. The local amplitude  $A_1$  of the leading transverse mode of the Fourier representation of bed elevation, scaled with its amplitude at the bifurcation is used to show the influence area of the bifurcation. The results are shown in Figure 2.3.

Figure 2.3 shows that the difference in bed elevation between the left and right river side, that will split into the two branches, quickly decreases in a non-linear way. No papers have been found that elaborate on the transverse mode or on the region upstream where the effects of the bifurcation are noticeable.

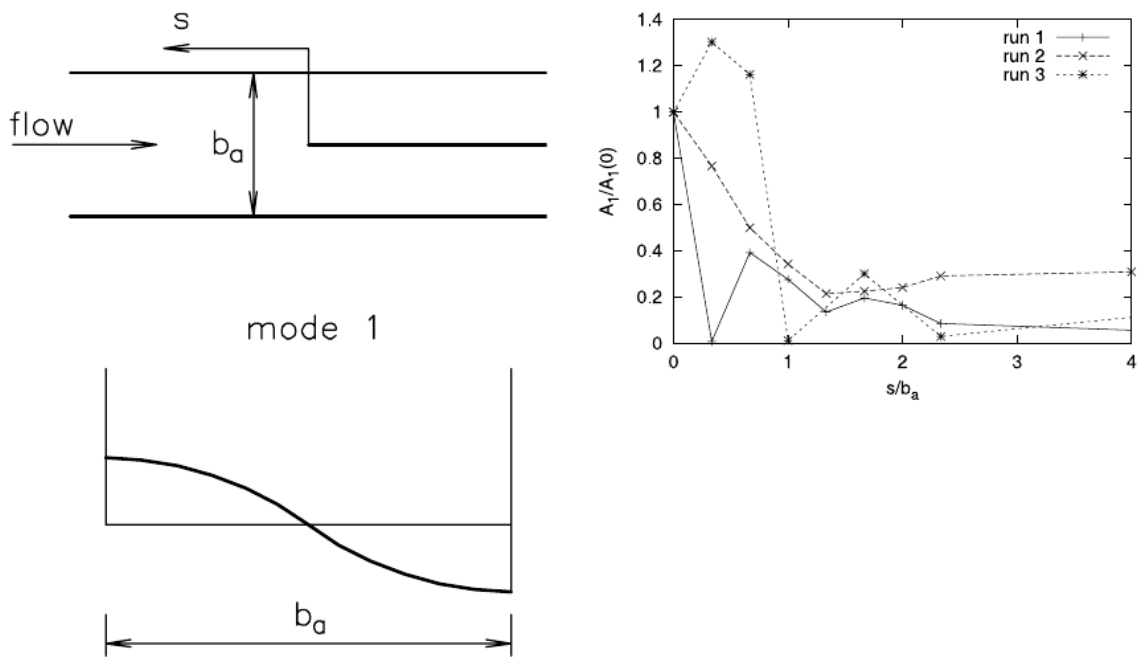


**Figure 2.3:** The amplitude of the first transverse mode of the Fourier representation of measured bed profile, scaled with its value at the nodal point, is plotted versus the dimensionless upward distance from the nodal point  $s/b_a$  ( $b_a = 0.6m$ ,  $d_s = 1.2mm$ ; *run1* :  $Q_a = 15.0l/s$ ,  $i_a = 0.002$ ; *run2* :  $Q_a = 24.9l/s$ ,  $i_a = 0.002$ ; *run3* :  $Q_a = 15.0l/s$ ,  $i_a = 0.002$ ). The transverse structure of the first Fourier mode is sketched in the lower left-hand part of the figure (Pittaluga et al., 2003)

### **2.2.3 Effect of sedimentation and erosion zones**

Bulle (1926), Kleinhans et al. (2013) and Zinger et al. (2013) show that the change in direction of the current due to the bifurcation results in flow separation zones. Here sedimentation will occur due to the lower flow velocity. However, no formulas have been found that enable a quantification of these zones and their effect on bathymetry. Dutta et al. (2017) have done 3D simulations investigating the Bulle effect. These simulations confirm the flow separation zones but predicting the location and size of these zones was difficult with the used RANS based model.

## **2.3 Conclusions**

The physics based model as developed by Zervakis (2015) gives a basis for the water depth in the upstream and downstream branches around a river bifurcation. This physics based model is based on the Chézy equation which is also used in Wang et al. (1995), Pittaluga et al. (2003) and Miori et al. (2006). Pittaluga et al. (2003) have found a relationship between upstream river width and upstream transition zone. No other quantitative relationships are found in the literature. Qualitative features of the bed level around a bifurcation are described in several papers, mostly based on the study of Bulle (1926). Here the occurrence of deposition zones due to flow separation is studied for bifurcations with varying.



# Methodology

This chapter will detail the methods that are used for this thesis study. First, the methods used to analyse the effect of various parameters on the bed level around bifurcations are explained. Then the methods used for the implementation of the tool are briefly discussed. Thirdly, the methods to determine the performance of the extended rapid assessment tool are provided.

## 3.1 Bifurcation analysis method

From the literature, few details about the transition zone can be derived. The river width is the only parameter that relates to the transition zone length according to the literature. The effect of other parameters is not analysed before. In order to obtain better understanding of the bed level at a bifurcation, the bed level data of several modelled bifurcations were analysed.

Simulations can be used to model many scenarios, many more than data of real river bifurcations is available. This makes it possible to analyse the effect of selected parameters on the bed level. However, the disadvantage is that these simulations can not take all factors in account that shape the river bed level. On this will be elaborated in Ch. 3.1.1. A schematisation method to schematise the bed level is introduced, as well as the method to validate this schematization method. Secondly, the methods to analyse the effect of four parameters on the transition zone length and bars and pools are shown. Finally, the method to analyse cross-sections are detailed.

In Figure 3.1 is a schematic river bifurcation shown. In this figure are the locations shown of where the profiles in the river are that will be analysed. In this figure is also the numbering of the branch shown which will be used in the rest of this study. Branch 0 is the main upstream branch, branch 1 the right branch downstream of the bifurcation and branch 2 the left branch.

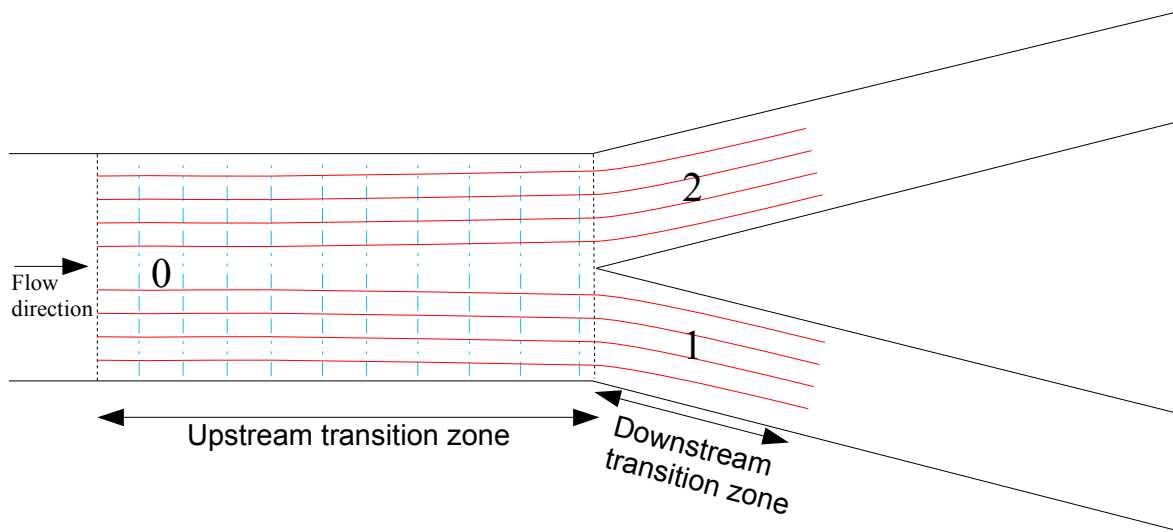


**Figure 3.1:** Schematic view of the bifurcation. The red (—) lines indicate the bed profiles in flow direction. The blue (.-.-) lines indicate which cross-sections will be studied.

### 3.1.1 Modelled data

In 2008, Maarten Kleinhans et al. have performed a study on the effects of river bends on the stability of river bifurcations (Kleinhans et al., 2008). For this study several scenarios of river bifurcations have been modelled using Delft3D FLOW. The varying of a single parameter per scenario makes this data set very suitable for this study. The river water depth output data from Kleinhans et al. (2008) have been used in this study. The data from these simulations will be referred to as modelled data in the rest of this study. The modelled data are an approximation of real situations. One limitation in the simulation is that the banks are fixed. This means that the river bed cannot change as freely as a real river. Another limitation relates to the discharge being constant throughout the entire simulation.

From the Delft3D FLOW manual: "Delft3D-FLOW is a multi-dimensional (2D or 3D) hydrodynamic (and transport) simulation program which calculates non-steady flow and transport phenomena that result from tidal and meteorological forcing on a rectilinear or a curvilinear, boundary fitted grid" (Deltares, 2014). Lesser et al. (2004) discusses the development and validation of the Delft3D FLOW. It is shown that Delft3D FLOW can be applied on analysis of real-life, prototype-scale situations. In Kleinhans et al. (2008), the sediment transport formula from Engelund and Hansen (1967) is used in the simulations. Instead of a real 3D model, a quasi 3D model is used. Ten vertical layers have been used that are coupled through hydrostatic pressure equation and a continuity equation for mass conservation. This allows for a grid with larger horizontal size than vertical size. The model is tested on the sensitivity on the used transport formulation, roughness and grain size. It is concluded that the overall behaviour of the bifurcation is not sensitive to the used transport formulation, roughness and grain size. The physics describing the movement of water and sediment has been implemented as good as possible in Delft3D FLOW and the methods used in the

Kleinhans et al. (2008) study. This will result in a modelled bed level that is close to a bed level that would follow from scale experiments and real cases. However, the limitations of the model have to be kept in mind when analysing the results of the analysis of the effect of a parameter on the transition zone.

Cross-sections of the water depth of the river have been made as well as water depth profiles in the flow direction. These both are based on the grid that is used to compute the water depth in the original model.

### 3.1.2 Schematization method

To analyse the modelled data, a method to schematise the water depth, of the modelled scenarios, is developed. This schematization is shown in Fig. 3.2a. The schematization is based on the assumption that upstream and downstream of the transition zone the water depth will be at its equilibrium depth. When the water depth starts deviating from this equilibrium depth the transition zone starts. When the water depth is back at its equilibrium depth the transition zone ends. The schematization consists of four points, points 1 and 4 indicate the beginning and the end of the transition zone. Points 2 and 3 indicate the bars and pools that occur in the transition zone. A visual inspection of the water depth in the modelled scenarios shows that these often occur.

To find the position of all four points that fits the best to the modelled data, all points have been varied. For every iteration only one single point has been altered. The points 1 is varied between zero and 4.5 times the upstream river width, away from the bifurcation. Point 4 is varied between zero and 3.5 times the width of the upstream river, away from the bifurcation. For both points this is done with steps of 0.25 times the width of the upstream river. Points 2 and 3 are varied horizontally between the bifurcation point and point 1 or 4 with steps of 0.25 times the width of the upstream river. They are also varied vertically according to:  $P2_y = P1_y + (P1_y - P4_y) * n$  and  $P3_y = P4_y - (P1_y - P4_y) * n$ . Here in is  $n$  varied between 0 and 0.6, with steps of 0.03, times the water depth difference of point 1 and 4. The Root Mean Square Error (RMSE, Ch. 3.3.3) is calculated for every iteration of this schematization. The iteration with the lowest RMSE represents the best fitting schematization and will be used for further analysis. The limits between which the points are varied are chosen such that the transition zone will be within the limits and the the bars or pools as well. Only when pools or bars are very shallow and long, points 1 or 4 are placed on the limits. Increasing the limits would result in computing times too long for this study.

The length of a bar or pool is defined as the distance between point 1 and 2 or point 3 and 4. The size of a pool or bar is defined as the difference in water depth between point 1 and 2 or point 3 and 4. A positive size value indicates a bar and a negative size value a pool. Because this method is created to incorporate bars and pools, it performs less well compared to the situation when there are no bars or pools. If there are no bars or pools, points 1 and 2 or points 3 and 4 will be nearly or exactly at the same water depth. When this happens, it can be assumed that the transition zone starts at point 2 and ends at point 3. Points 1 or 4 will be ignored in the analysis of that time step. This is done when the water

depth of the points 1 and 2 or 3 and 4 are within 10 cm of each-other. This threshold of 10 cm is based on the scale of the whole simulation and the size of the bars and pools that occur.

### Validation of methods

The schematization method is validated with a visual inspection. This is done for all used time steps. The location of the start and end of the transition zone is compared to the visually determined start and end. The location of the points 2 and 3 are compared with the location of the peaks of bars and troughs of bars.

### 3.1.3 Analysed parameters

Four category of parameters of the bifurcation were analysed: i) the difference in water depth between the start and end of the transition zone, ii) the discharge distribution, iii) the width of the upstream and downstream river, and iv) the upstream river bend radius. Finally, the effect of the transition zone on the bars and pools, as well as, the relation between the bar and pool length and their size is analysed. These parameters have been selected because they can be derived from scarce data. Width and bend radius can be derived from satellite images, the equilibrium water depth at the beginning and end of the transition zone can be computed based on discharge, slope, width and an estimation of the Chézy coefficient. The discharge and discharge distribution are required to be known for the cases that are assessed on the basis of the extended rapid assessment tool. In the following sections the analysis of each of these parameters will be elaborated on.

#### i) Difference in water depth between start and end of the transition zone

The difference in water depth at the begin and end of the transition zone is one of the most important parameters that determines the river bed level in the transition zone. Zero change

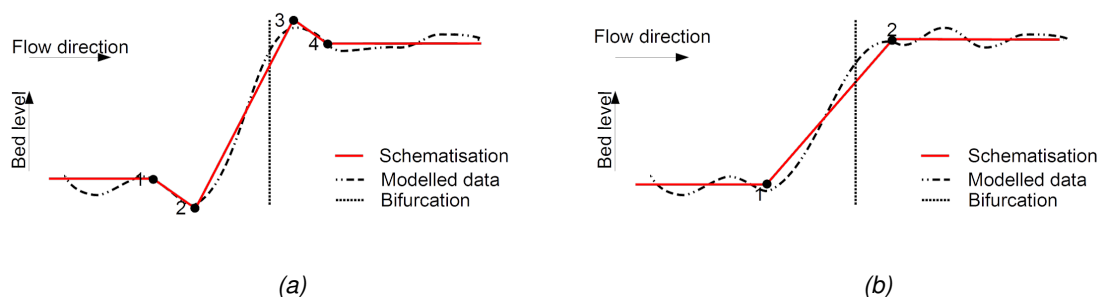


**Figure 3.2:** Schematization used for determination of transition zone length. (a) Point 1 and 4 indicate begin and end of transition zone, point 2 and 3 indicate the bars and pools. (b) Simplified schematization method, point 1 and 2 indicate the beginning and end of the transition zone

in water depth at the upstream versus downstream levels means that the bed level will be as good as flat and there is no transition zone.

The modelled data from the Kleinhans et al. (2008) study is used as source of data for this analysis. In the modelled simulations the discharge distribution shifts from an equal distribution to a situation where almost all discharge flows into one of the branches. This leads to considerable differences in water depth between the upstream and downstream of the transition zone, as well as, between the two downstream branches.

### **ii) Discharge distribution**

The change in discharge distribution is closely related to the change in water depth. Since the values for width and slope are fixed in the model, the water depth will have to increase in order to let discharge increase. The effect of the discharge distribution on the transition zone will be analysed in a similar method as is used for the analysis of the effect of water depth on transition zone.

### **iii) River width**

According to the literature the width of the upstream river is a determining factor for the length of the upstream transition zone. In this analysis it will be assessed whether this also holds true for the modelled data. Similarly, the relationship between downstream river width and total or downstream transition zone length is assessed. From the modelled data, only those scenarios with varying river width, are used. The length of the transition zone of all time steps is shown in a box plot per scenario.

### **iv) Upstream river curvature**

The effect of upstream river curvature ( $\gamma$ ) on the transition zone is determined using scenarios with varying curvature. In these scenarios the curvature is increased from a bend radius of 100 times the width of the upstream river to only four times. The length of the transition zone of all time steps is shown in a box plot per scenario.

### **v) The transition zone**

The effect of the transition zone itself on the bars and pools is studied. This is performed by plotting the bars and pools length with respect to the transition zone length as well the bars and pools size with respect to the transition zone length. A trend line is fitted to the data. Finally, the relation between bars and pools length and their size is studied. This is done by plotting the size with respect to the length and fitting a trend line to this data.

## **3.1.4 Cross-sectional profiles**

The analysis of the profiles in flow direction gives only limited insight in the difference between the right side and the left side of the river upstream of the bifurcation. In addition

to the profiles in flow direction, cross-sectional profiles are also studied. The transition in the cross-section between the left and right side of the river is described for the upstream transition area. Here, the difference in water depth between the left side and the right side of the river will be the largest. The cross-sections will only be described qualitatively.

## 3.2 Implementation

The extension of the rapid assessment tool is done in two steps. The first step is the creation of the grid, of the river, and the second step is the implementation of the found relationships to approximate the river bed level. The method to create the grid is based on the paper of Amsden and Hirt (1973). The grid is moved into the correct position in an automated iterative way. In Ch. 5.1 the creation of the grid will be more elaborated upon.

The computation of the river bed level is based on interpolation between the begin and end of the transition zone. Four types of interpolation are implemented. Firstly, a single step method in bed level at the bifurcation is implemented, herein is no transition zone present. The bed level has a sudden jump between the upstream bed level and the downstream bed level. Next the bed level will be linearly interpolated between the beginning and end of transition zone. Interpolation using a Gaussian error function is the third method of interpolating. Finally the bed level will be computed using linear interpolation method but with bars and pools included. A more elaborate description of the methods used in the implementation of the extended rapid assessment tool is given in Ch. 5.2.

## 3.3 Evaluation method

The accuracy of the extended rapid assessment tool will be determined in the last phase of this study. Three case studies will be performed in order to assess the accuracy. To this end, a qualitative method and a quantitative method will be used. The qualitative method is based on a visual inspection of the results in relation to available high accuracy bed level data of the river. The Root Mean Square Error (RMSE), between the modelled bed level and the high accuracy bed level data, will be the quantitative method. Both methods will be further discussed in this chapter.

To evaluate the accuracy of the interpolation methods, two methods are used to set the bed level up and downstream of the transition zone. The first method is to compute the bed level with the physic based model. The other method is to use the measured bed level for these areas. The first method will give insight in the over all performance of the extended rapid assessment tool. The second method will give insight in how well the various interpolation methods perform.

### 3.3.1 Transition zone

The transition zone is determined for measured data by using a simplified schematization method based on the method described in Ch. 3.1.2. Potentially present bars and pools are not taken into account, points 2 and 3 are not included in this schematization. The reason for this is that the bed level have large local variations which led to false estimations of the transition zone length when applying the unsimplified method.

### 3.3.2 Visual evaluation

The bathymetry data computed by the extended rapid assessment tool will also be assessed visually. To this end, an error map will be created. Here the difference between the computed bathymetry and the real bathymetry will be shown. This will allow a direct visualisation of tool-based errors that occur in specific locations at the river bifurcation site.

### 3.3.3 RMSE

The river bed level data generated by the extended rapid assessment tool are compared with high accuracy measured data in order to assess it accuracy. The method used by Zervakis (2015) to evaluate the accuracy of the rapid assessment tool is the RMSE method. This method is also used in numerous other studies regarding evaluation of elevation data (Wood and Fisher, 1993), (Kenney and Keepings, 1962). The RMSE is calculated according to Eq. 3.1.

$$RMSE = \sqrt{\frac{\sum_{i=1}^n (\hat{v}_i - v_i)^2}{N}} \quad (3.1)$$

where:

$N$  = number of samples

$\hat{v}$  = real value at  $i$

$v_i$  = predicted value at  $i$



# Bifurcation analysis

In this chapter the bathymetry around river bifurcations will be analysed. This will be done with data from a Delft3D model. This model will be introduced first. Then the schematization method, as described in Ch. 3.1.2, for the schematization of the modelled water depth, will be validated. The effect of four parameters on the transition zone is analysed.

## 4.1 Modelled data

In 2008 Kleinhans et al. have performed a set of simulations to investigate the effect of bends on the stability of bifurcations. The water depth data generated for their study are used in the present study. The most important parameters used for the modelling will be summarized here. The details of the settings used for the modelling can be found in Kleinhans et al. (2008). Thirteen scenarios from the Kleinhans et al. study have been used. In the first seven scenarios the river bend radius has been varied between two and 100 times the upstream river width. In scenario 8 to 10 the width of branch 0 been varied between 288 m and 630 m. In scenario 11 to 13 is a combination of varied bend radius and increased slope in branch 2. Here the slope is 0.11 m/km. A description of every scenario can be found in Appendix A.

The two standard grids, on which the water depth is computed, are shown in Figure 4.1. The grid consists of 80 by 20 cells and 10 layers were used to create a 3D grid. A standard cell is 150 m long and 28 m width. The radius of the downstream bend is set at 20 times the width. The default slope is 0.1 m/km and the discharge is 2500 m<sup>3</sup>/s.

The whole simulation covers 263.000 minutes of water movement using time-steps of 0.5 minutes. It has an initialization time of 200 minutes for the water movements. The morphological factor used was 100, this translates to a real timespan of 50 years. The state of the simulation was saved every 2000 time-steps, resulting in 251 saved time-steps. In all scenarios it takes at least 80.000 minutes before a significant change in bed level around the bifurcation develops. Only the time-steps after a change in bed level is noticeable, are taken into account in all analyses. Further reference will therefore be to this selection of time-steps after the initial change.

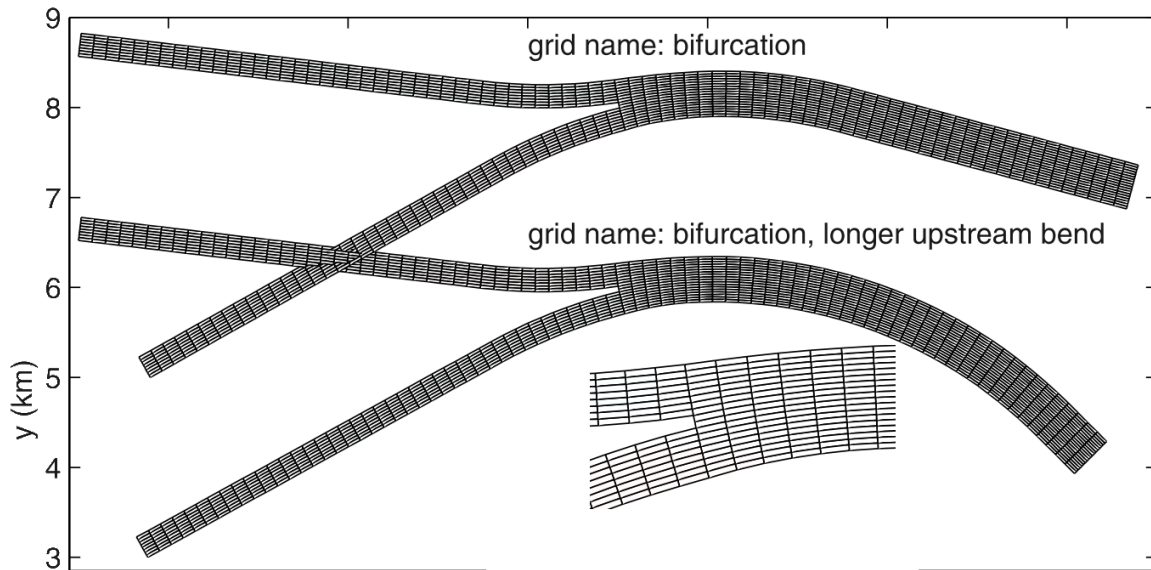


**Figure 4.1:** The grid used in the simulations performed by Kleinhans. The grid consists of 20 vertical cells and 80 horizontal cells.

#### 4.1.1 Validation schematization method

The schematization method is validated for all time steps by using visual inspection. The transition zone is visually determined and compared with the transition zone as determined by the schematization method. One time step of scenario 5 is shown in Figure 4.2. Here, the profile is shown in flow direction of the centre of both branches. Branch 1 is downstream of the bifurcation deeper than upstream. The schematization seems adequate. The bars and pools are correctly placed at the beginning and end of the transition zone. For branch 2 the method does not work as well. Here a sandbank forms at the beginning of the branch. Over time this bank grows into the branch. This results in a shallow part in the beginning of the branch 2 followed by a deeper part downstream of the branch. This is not an equilibrium situation and also not within the limits for the schematization method to be applied. To still be able to use the method, point 4 has been given the same location as point 3. This means effectively that the transition zone length is defined by the location of point 1 and 3 and that any pools or bars that would occur downstream of the transition zone, in a branch that dries out, are not taken into account in this analysis.

For most of the profiles the computed schematization is stable for the whole simulation. Only small shifts of the location of the points take place. For some of the profiles, however, the location of the points can change every few time steps between 2 locations that are far apart. This jumping between two locations causes extra spreading in the transition zone length. The schematization method can be improved to give more stable schematization of the bed level. One way that could achieve this is by using smaller steps for finding the best location for the points. Another way could be by basing the schematization on the schematization of the previous time step.

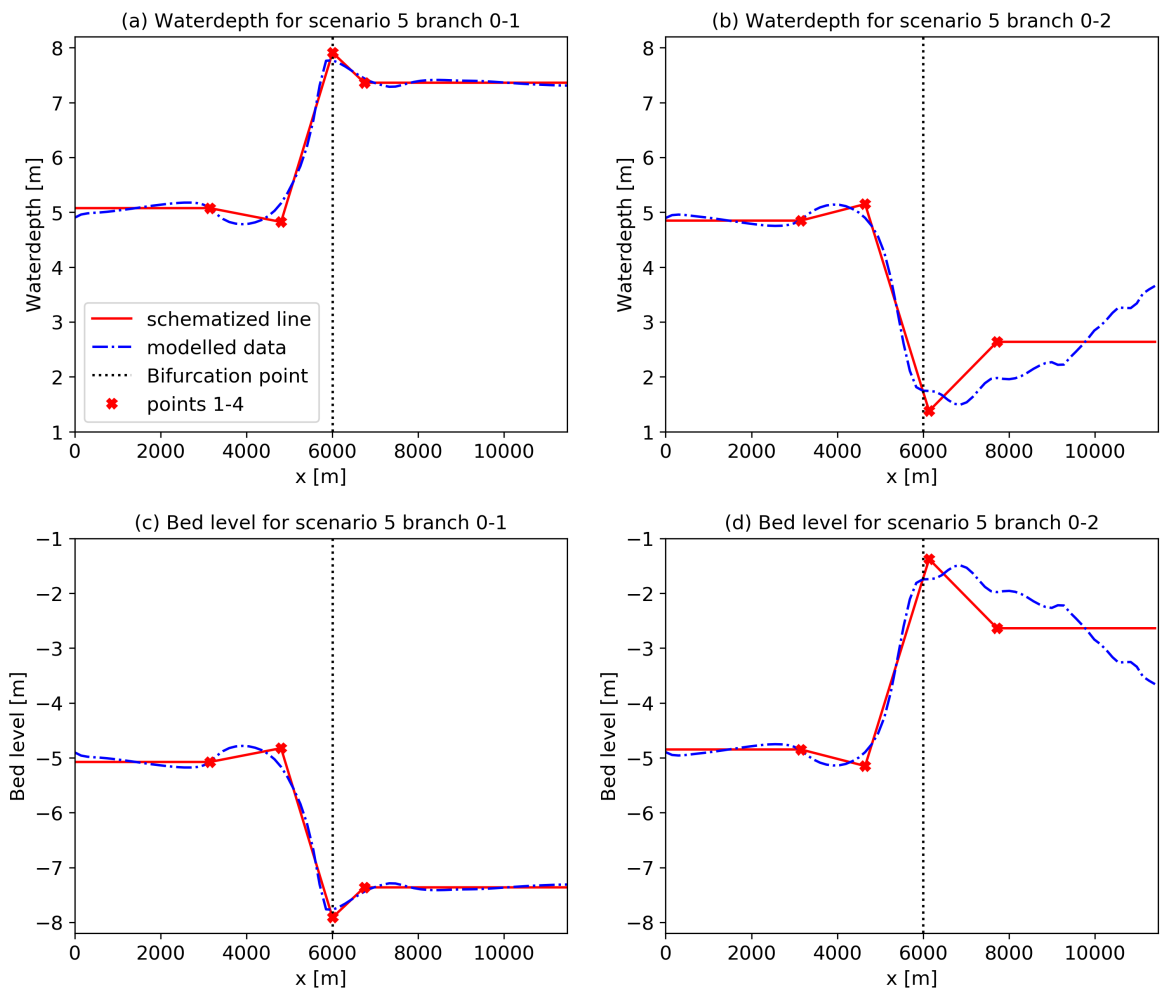


**Figure 4.2:** Profile in flow direction of the water depth (a,b) and the bed level (c,d) at the centre of branch 1 (a,c) and 2 (b,d) of scenario 5 halfway the simulation. The schematization, including all four points is shown here as well. The flow direction is in positive x direction.

## 4.2 Analysis of the effect of parameters on the transition zone

### 4.2.1 The effect of difference in water depth on the transition zone

In Figure 4.3 the change in water depth between start and end of the transition zone with respect to the length of the upstream and downstream transition zone, is shown. A positive  $\Delta W D$  means that the water depth in branch 1 is higher than in branch 0. There is no obvious relationship between the difference in water depth and the upstream or downstream transition zone length. The  $R^2$  of the fitted trend line is only 0.03 which indicates a very poor correlation. The  $R^2$  of the trend line fitted to the difference in water depth and the downstream transition zone length is higher; it is 0.44. This is still not very high. The trend line has an interesting slope and start length. The line indicates that at a zero difference in water depth, there is still a transition zone of 700 m. For a difference in water depth of -5 m the transition zone is 0 m according to the trend line.

These values do, most probably, not agree with reality. When there is no difference in the water depth upstream and downstream of the bifurcation, there would be no transition zone. When the difference in water depth would be larger than -5 m there would be a negative transition zone length, which is not possible. The relationship found here can be specific for the type of bifurcation that is used in all scenarios. The found relationship cannot be applied to any other bifurcations where, for instance, discharge and river width are different from these in the scenarios.

### 4.2.2 The effect of discharge distribution on the transition zone

In Figure 4.4 the transition zones lengths are shown with respect to the discharge distribution. Just as in Figure 4.3 are the modelled data rather dispersed. The  $R^2$  of the trend lines are only 0.00 and 0.21, indicating a poorer fit than the trend line for the effect of the water depth. However, the discharge distribution on all rivers has a range from zero to one. This would mean that the relationship can be applied to any river bifurcation.

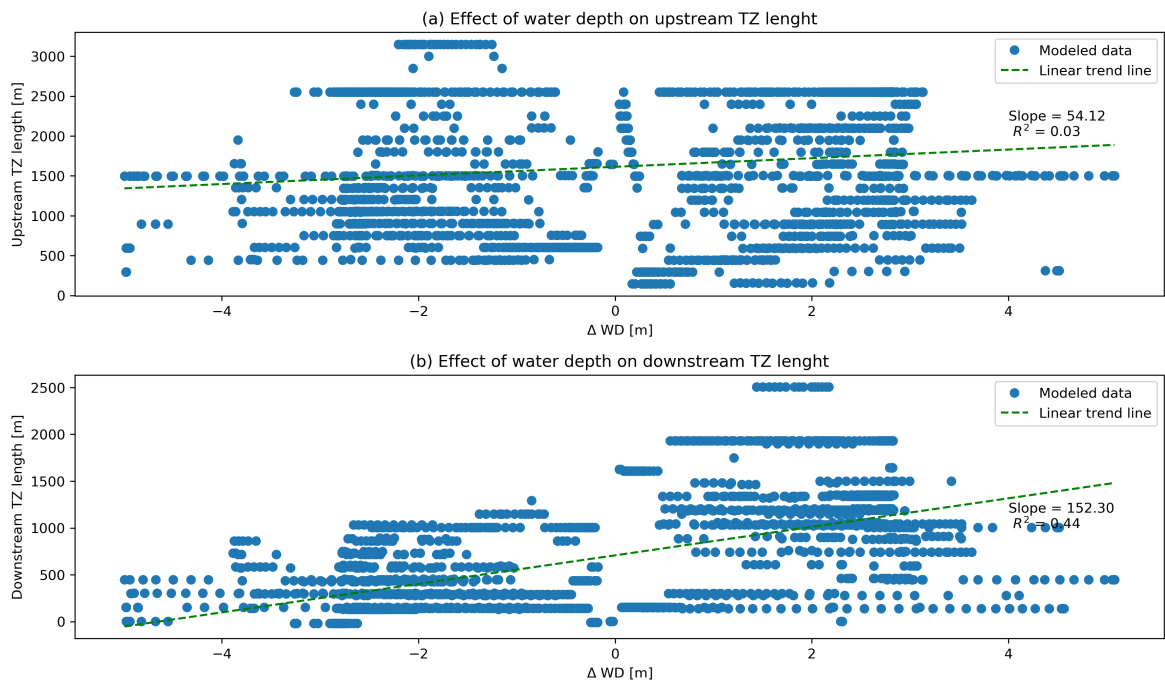


**Figure 4.3:** Difference in water depth plotted with respect to the upstream and downstream transition zone length for all time steps of all scenarios. The trend line is fitted to the data.

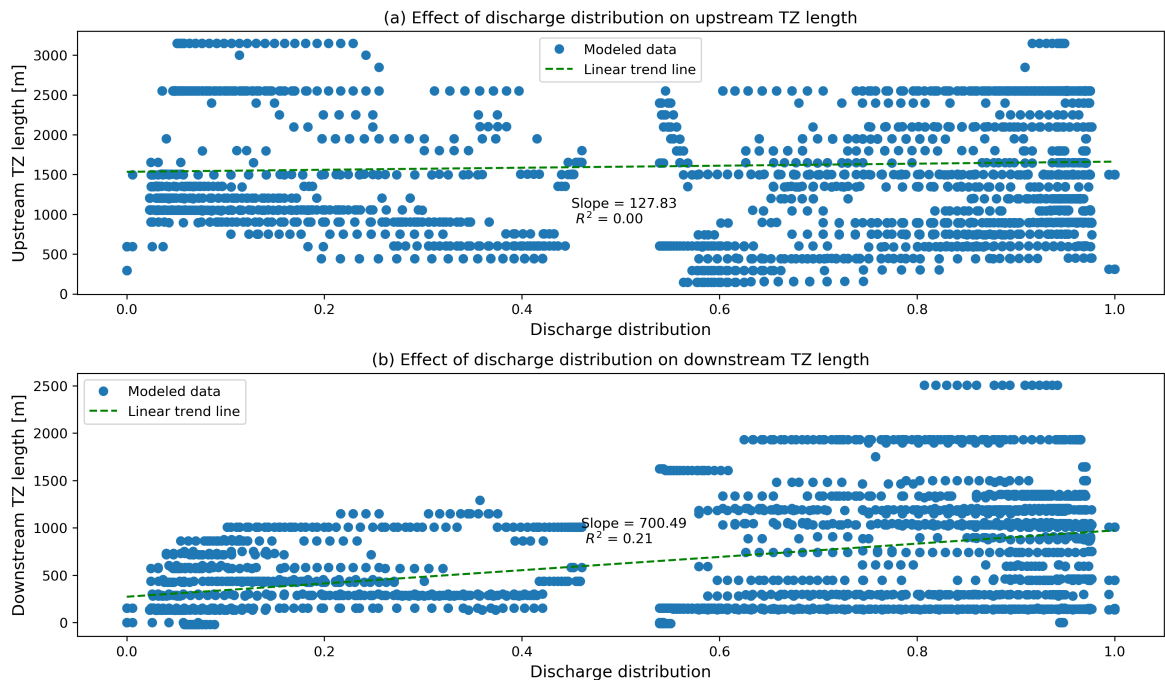


**Figure 4.4:** Discharge distribution plotted with respect to the upstream and downstream transition zone length for all time steps of all scenarios. The trend line is fitted to the data.

### 4.2.3 The effect of river width on the transition zone

The literature already indicated a relationship between the upstream river width and the upstream transition zone length. The upstream transition zone length is plotted with respect to the upstream river width in Figure 4.5. A linear trend line is fitted to these data. The slope of this line is 2.55 and the  $R^2$  of this line is 0.22. This indicates a bad fit of the trend line, and thus a weak correlation between the two parameters. The downstream transition zone length is plotted with respect to the the downstream river width. Because the downstream river width is equal to half the upstream river width, the effect of the upstream river width on the transition zone is equal to the effect of the downstream river width. Based on the available data it is not possible to determine whether the upstream river width has a different effect on the downstream transition zone length compared to the downstream river width has. The  $R^2$  of the fitted trend line is only 0.09, indicating a very weak correlation.

### 4.2.4 The effect of upstream curvature on the transition zone

In Figure 4.6 the curvature of the upstream river is shown with respect to the beginning and end of the transition zone. There is a relatively good correlation, but still weak, between the start of the transition zone and the radius of the upstream river bend. The  $R^2$  of the trend line is 0.22 as well. Between the downstream transition zone length and river curvature there seems to be no relation. The low slope and  $R^2$  value of the trend line confirm this.

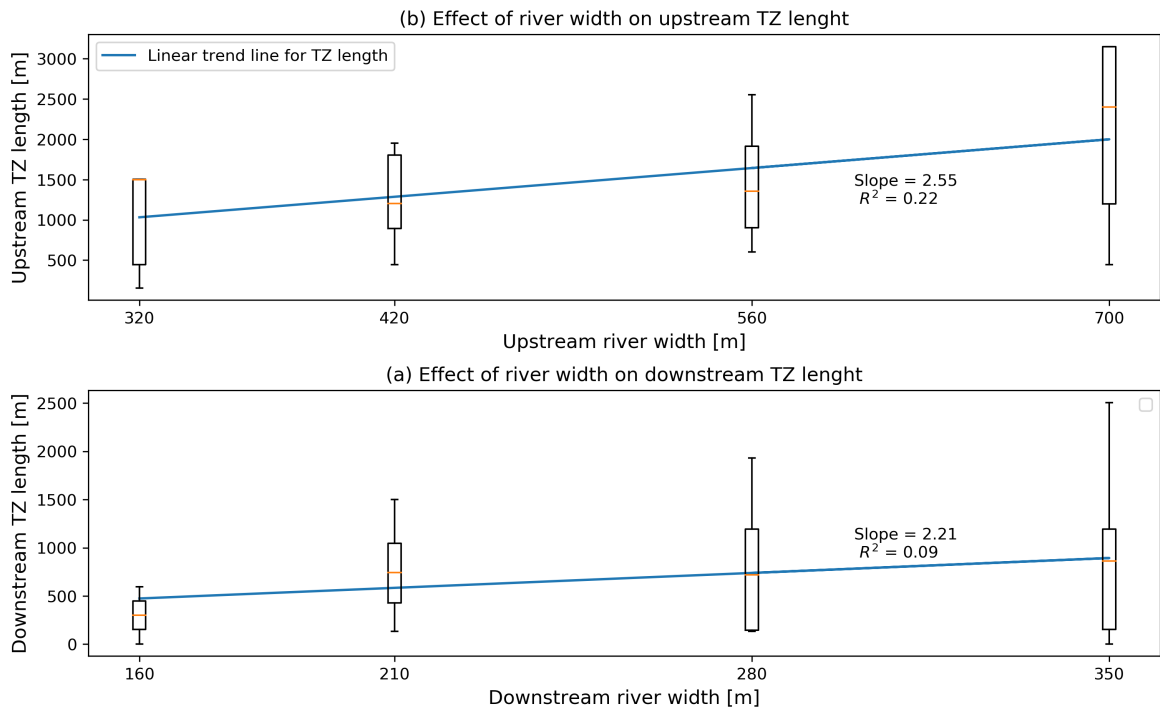


**Figure 4.5:** The river width shown with respect to the average transition zones length of the modelled data per scenario. The linear trend line is fitted to this data.

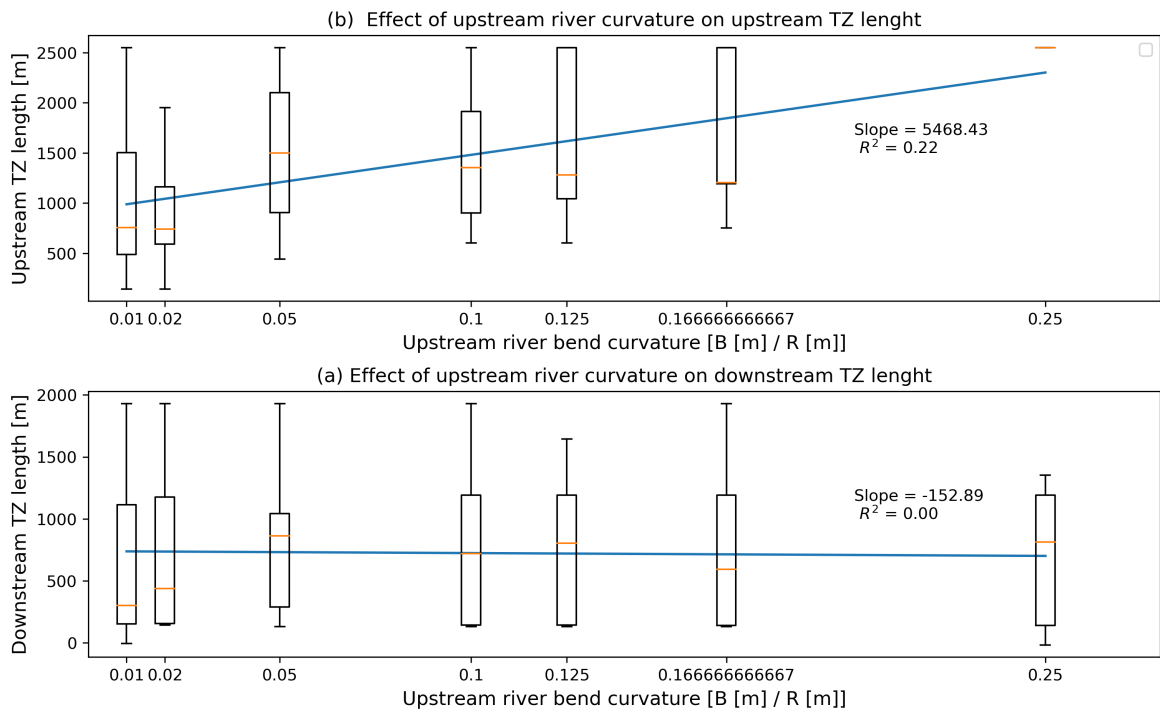


**Figure 4.6:** Change in upstream river curvature shown with respect to the average transition zones length of the modelled data per scenario and the measured data. The linear trend line is fitted to these data.

### 4.2.5 The effect of difference in water depth on bars and pools

In Figure 4.7 the change in water depth between the start and end of the transition zone shown with respect to the length and size of the bars and pools, is shown.

The bars and pools are shown per branch. Branch 2 has only an upstream bar or pool because the downstream bar or pool is not taken into account, as is explained in 3.1.2. The points are very dispersed, this indicates that there is no relation between the difference water depth and the bars or pools. The low  $R^2$  of all trend lines supports the non existence of a relation between difference in water depth and bars or pools.

### 4.2.6 The effect of river width on bars and pools

In Figure 4.8 the bar and pool length and size are shown with respect to the river width. Where the upstream transition zone length had a good correlation with the upstream river width, this seems not to be the case for the bar and pool length. Between the downstream river width and the size of the downstream pools or bar there does seem to be a relation. The trend line fitted to the data has a high coefficient of correlation: the  $R^2$  of 0.93 indicates a good fit of the trend line to the data. The trend line for the relation between the size of the bar or pool and the river width has a  $R^2$  of 0.80, indicating a good fit.

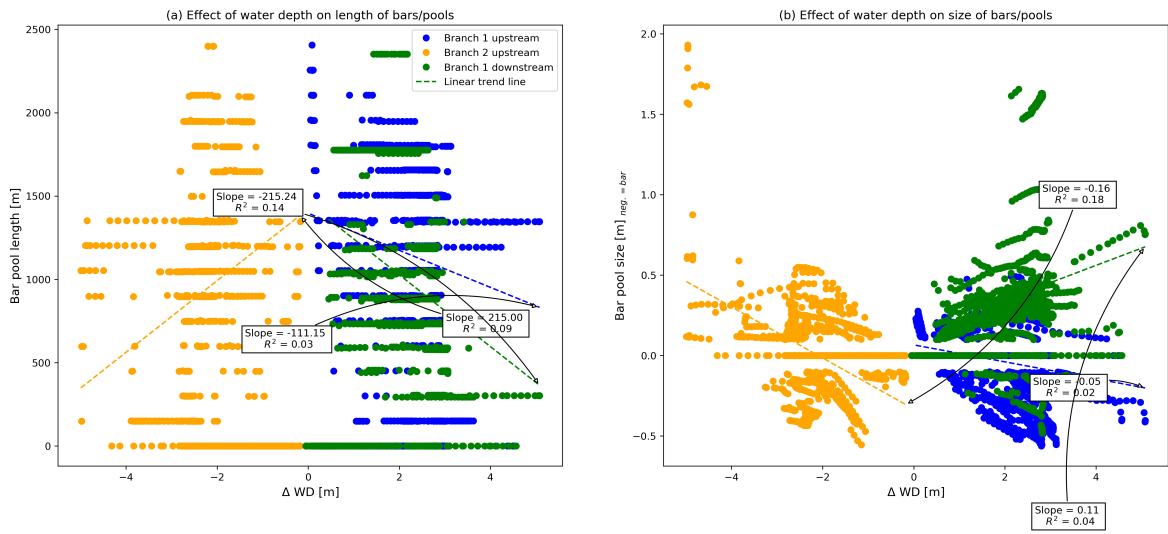


**Figure 4.7:** Difference in water depth plotted with respect to (a) the bar/pool length and (b) the bar/pool size, for all time steps of all scenarios. The trend line is fitted to these data.

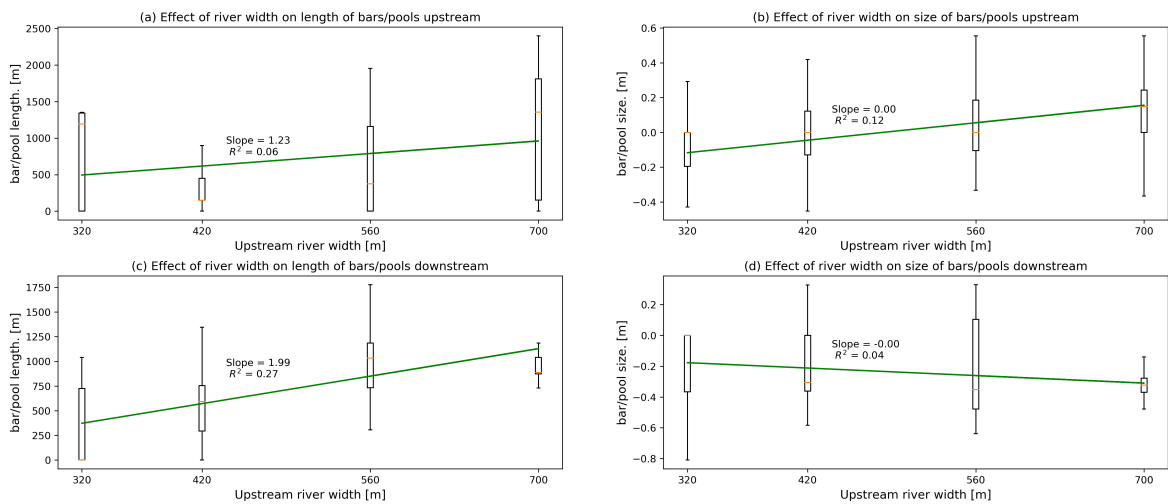


**Figure 4.8:** The river width shown with respect to the bar pool length (a) and size (b) of the modelled data per scenario.

### 4.2.7 The effect of upstream river curvature on bars and pools

In Figure 4.8 the bar and pool length and size are shown with respect to the upstream river curvature. Just as with the transition zone length, a relationship is observed. The relationship between curvature and the size of bars or pools is quite strong for the downstream bars or pools. The relationship with the upstream bars and pools size is weaker. For sharper bends the bars and pools, both upstream and downstream, are larger.

### 4.2.8 The effect of the transition zone length on bars and pools

The relation between the transition zone length and the length and size of bars and pools is also investigated. The results are shown in Figure 4.10. A clear correlation between the length of the transition zone and the length of the bars and pools is found. The  $R^2$  of the trend line for the upstream bar or pool length is 0.70 and for the downstream bar or pool length is 0.64.

There is no clear relation between the length of the transition zone and the size of a bar or pool is no clear relation. For both trend lines the  $R^2$  is almost zero.

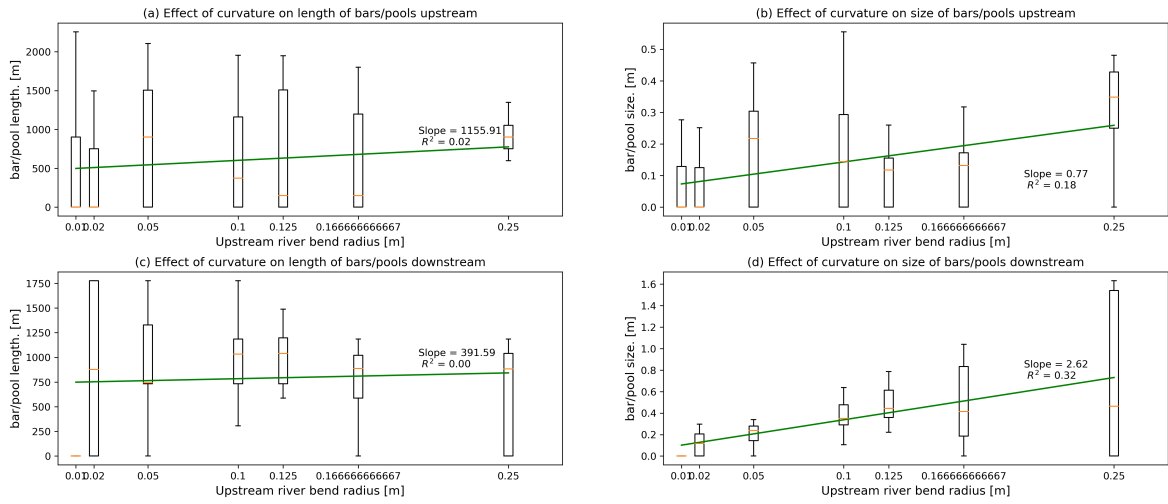


**Figure 4.9:** The upstream river curvature shown with respect to the bar pool length (a) and size (b) of the modelled data per scenario.

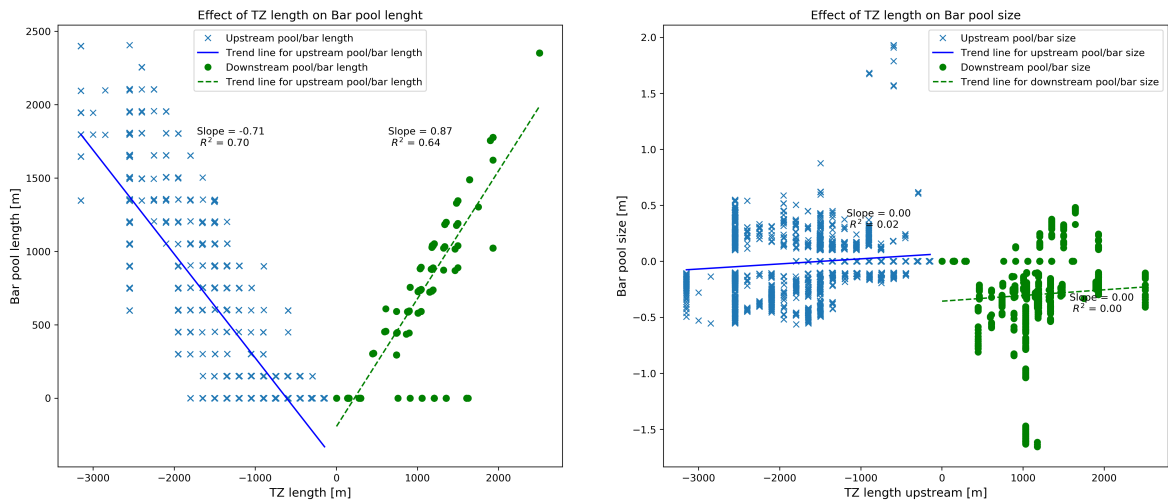


**Figure 4.10:** The transition zone length shown with respect to the bar pool length (a) and size (b) of the modelled data per scenario.

### 4.2.9 The effect of bar or pool length on the size of bar or pool

The length of the bars or pools has no effect on their respective size according to the trend line fitted to the data. This is shown in Figure 4.11. The coefficient of correlation for both upstream and downstream pools and bars is nearly zero.

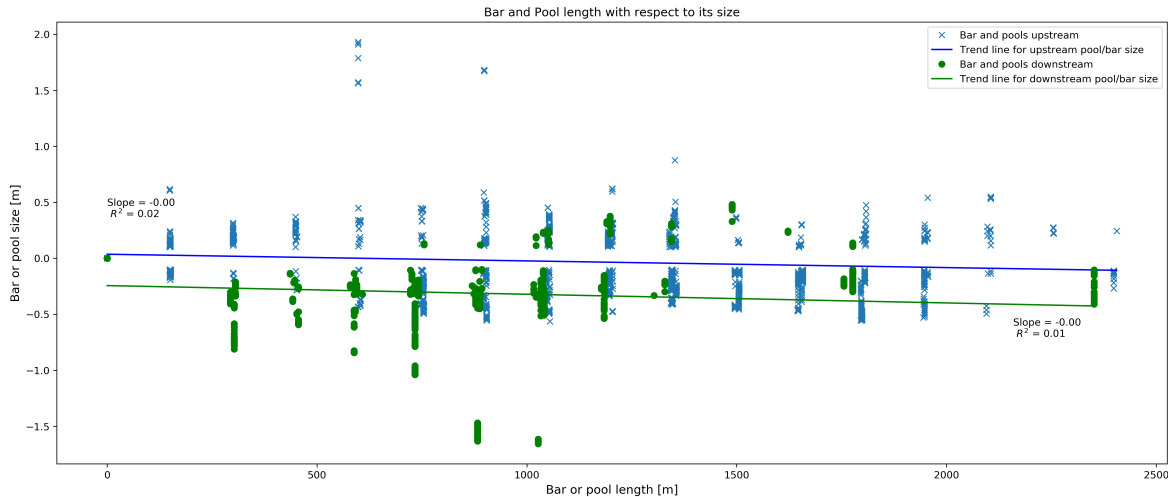


**Figure 4.11:** The bar and pool length shown with respect to the bar pool size of the modelled data.

## 4.3 Cross-sectional profiles

In Figure 4.12 are several cross-sectional profiles shown of scenario 1 at the end of the simulation. Cross-section 11 is the last full cross-section before the bifurcation. All cross-sections show a smooth transition between the left and right side of the river. This continues up to the bifurcation. The transverse slope due to the curvature of the river is clearly visible. The first cross-section does not show this transverse slope due to the boundary conditions of the model. The other scenarios have been studied too and show similar results.

## 4.4 Conclusions

In this section the conclusions that are relevant for the implementation of the found relationships, in the extended rapid assessment tool, will be discussed. Other conclusions will be discussed in Chapter 8.1. The combination of the upstream river width and the upstream river curvature can be used to predict the length of the upstream transition zone. This is performed with Eq. 4.1. The other parameters that are analysed have no relation with the upstream transition zone length.

$$TZ_{upstream\ length} = 5468\gamma + 2.55W_{upstream} - 494 \quad (4.1)$$

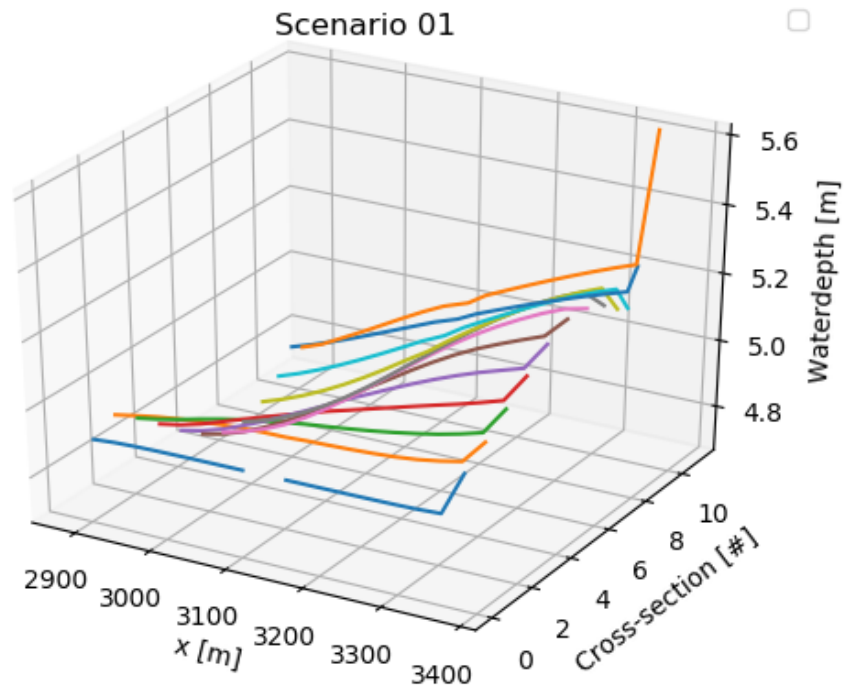


**Figure 4.12:** The water depth upstream of the bifurcation for scenario 1 at the end of the simulation. Cross-section 0 is at the start of the grid, cross-section 11 is just upstream of the bifurcation

where:

$\gamma$  = Upstream river curvature [-]

$W$  = River width [m]

The difference in water depth has the strongest correlation with the downstream water depth. However, the water depth has a direct relation with discharge and river width. The analysis indicates that there could be a relationship between difference in water depth and downstream transition zone length but the found parameters for the slope and y-intercept are specific for the analysed bifurcation. Therefore, it is not suitable for implementation in the extended rapid assessment tool. The trend line of the discharge distribution has the second highest  $R^2$  for predicting downstream transition zone length. Applying this relation would result in equal downstream transition zones even when bifurcations are very different. The relations for the upstream transition zone length are related to the geometry of the bifurcation, this aspects misses when the downstream transition zone length would only be determined by the discharge distribution. The analysis does show that a relation between discharge and transition zone might exist. Because the first two relationships seem unfit for estimating the downstream transition zone length, the third relationship is selected to be

used. This is the relation between downstream river width and the downstream transition zone length. Because there is a direct relation between upstream and downstream river width as used in the model, it cannot be determined whether either of the relations between the upstream river width or downstream river width and the downstream transition zone length is better in practice. The downstream transition zone length is described with Eq. 4.2.

$$TZ_{downstream\ length} = 2.21 * W_{downstream} + 121 \quad (4.2)$$

The bars and pools occurring in the transition zone are difficult to quantify with the selected parameters. There are sometimes no bars or pools in the transition zone. A relation between upstream river curvature and downstream bar or pool length and size is detected. The other strong relation identified is between the transition zone length and the bar or pool length. However, there is no relation between the transition zone length and the bar or pool size. There is also no relation between the bar and pool length and their respective size. The bar or pool length can be described with Eq. 4.3 and 4.4, the size can be described with Eq. 4.5 and 4.6.

$$Bar\ or\ pool\ length_{upstream} = 0.71 * TZ_{length\ upstream} - 434 \quad (4.3)$$

$$Bar\ or\ pool\ length_{downstream} = 0.87 * TZ_{length\ downstream} - 195 \quad (4.4)$$

$$Bar\ or\ pool\ size_{upstream} = 0.77\gamma - 0.07 \quad (4.5)$$

$$Bar\ or\ pool\ size_{downstream} = 2.62\gamma - 0.08 \quad (4.6)$$

The cross-sectional profiles show a smooth transition between left and right bank. No indication of the coming bifurcation can be seen in the last cross-section. The transition between the beginning and end of the transition zone is also a smooth transition. Upstream and downstream of the transition zone the water depth is at equilibrium water depth. In most scenarios bars and pools occur upstream and downstream of the bifurcation point.

# Implementation

The methods that are used in the implementation of the extended rapid assessment tool are explained in this chapter. First the construction of the grid for the bifurcation, on which the bed level will be computed, will be explained. In the second part of this chapter the implementation of the relationships between the parameters and the transition zone length or the bars and pools as presented in Chap. 4 is shown.

## 5.1 Grid construction

The grid is the basis for the computation of the river bed level around the bifurcation. Based on the paper of Amsden and Hirt (1973), a method to create a grid for river bifurcation sites has been developed. The technique described in this paper allows to create grids in a great variety of shapes. It uses an iterative process to compute the location of the vertices. The method, as described in this paper, is adjusted to better fit to the purpose of this study. Two steps are required to create the grid. The first step creates a grid where the corner points are at the desired locations. The second step moves the borders to the desired locations.

A polygon of the river bifurcation is the basis for the final grid. From this polygon the orientation of the grid, location of corner vertices and, location of border vertices is derived.

The grid starts in a rectangular shape, the middle rows on j-axis, 6 and 7 in the example in Figure 5.1, have the same coordinates. In iterations the corner vertices of the grid are moved to their final position. The corner vertices are moved according to Eq. 5.1. In this equation  $x_0$  and  $y_0$  are the coordinates to where the vertex is moved. The other vertices are moved according to Eq. 5.3. For vertices at the border the equation will slightly change: in this case only directly connected border vertices are taken into account. The factor  $\frac{1}{8}$  is changed to  $\frac{1}{2}$ .

$$\begin{aligned}x_{new} &= x + \beta(x_0 - x) \\y_{new} &= y + \beta(y_0 - y)\end{aligned}\tag{5.1}$$

where

$$\beta = \beta_0[(x - x_0)^2 + (y - y_0)^2]\tag{5.2}$$

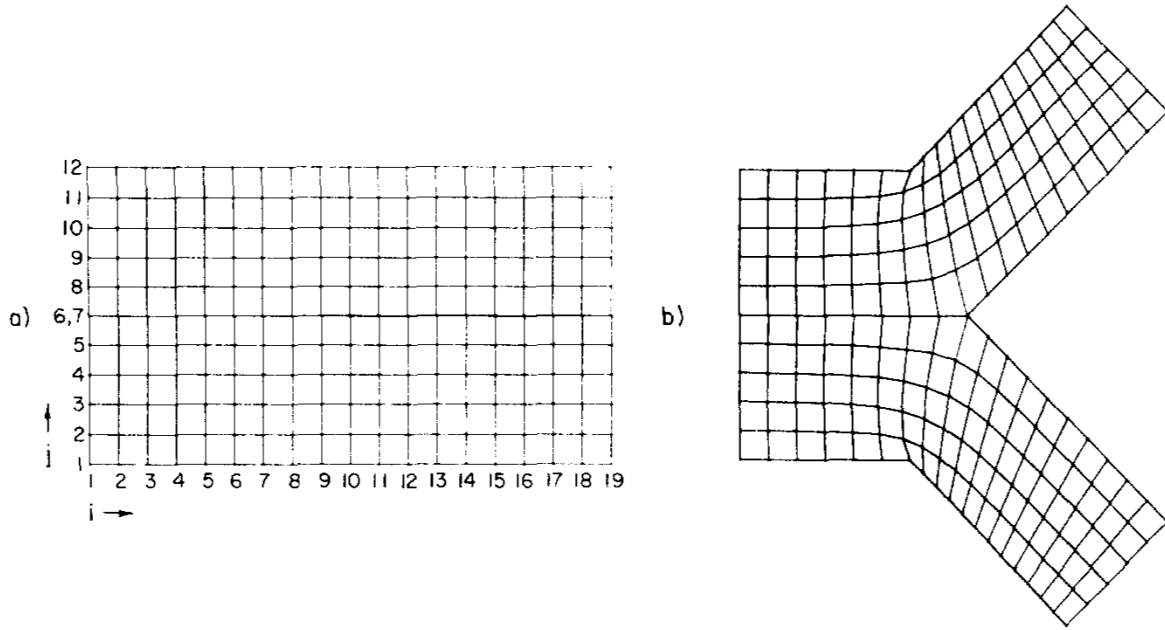


**Figure 5.1:** Example of transformation of a grid. source:(Amsden and Hirt, 1973) (a) the basis grid (b) the grid after the iterations

$$\begin{aligned}
 (x_i^j)_{new} &= \frac{1}{8}(x_{i+1}^j + x_{i+1}^{j+1} + x_i^{j+1} + x_{i-1}^{j+1} + x_{i-1}^j + x_{i-1}^{j-1} + x_i^{j-1} + x_{i+1}^{j-1}), \\
 (y_i^j)_{new} &= \frac{1}{8}(y_{i+1}^j + y_{i+1}^{j+1} + y_i^{j+1} + y_{i-1}^{j+1} + y_{i-1}^j + y_{i-1}^{j-1} + y_i^{j-1} + y_{i+1}^{j-1})
 \end{aligned}
 \tag{5.3}$$

In Fig. 5.1 an example is shown of a grid before and after the iteration according to the method described in Amsden and Hirt (1973). The grid lines in the middle of the grid in horizontal direction ( $j=6,7$ ) split at the bifurcation point.

When the corner vertices are in the correct position, the borders of the grid are aligned with the river banks. This is done by applying Eq. 5.1 to all vertices in the border. The  $x_0$  and  $y_0$  are the coordinates for the point on the polygon that is closest to the current location of the vertices. The result of the two steps can be seen in Fig. 5.2.

A more detailed description of the method used to create the grid can be found in Appendix B. This grid is only made to be used within the extended rapid assessment tool. The properties of the grid, like orthogonality, are of less importance for the application in the extended rapid assessment tool.

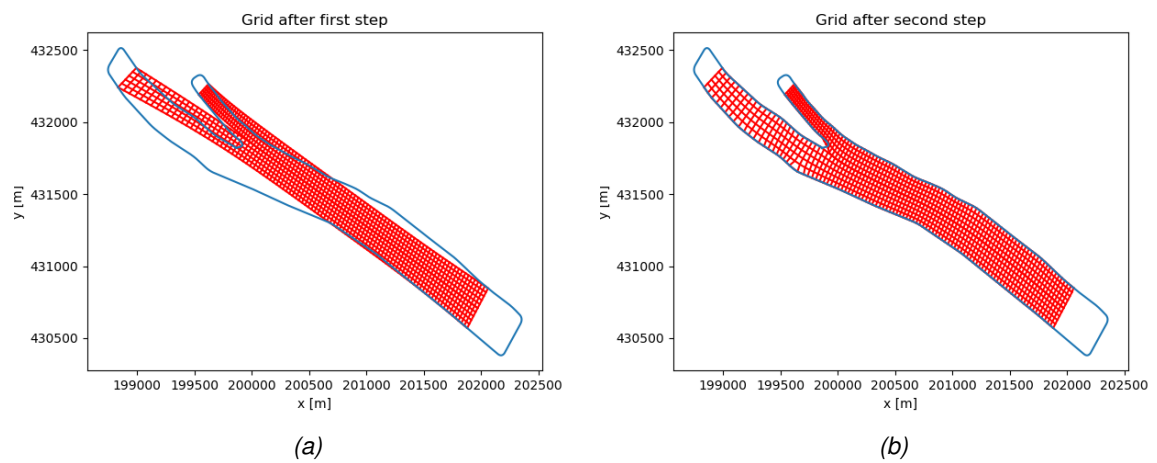


**Figure 5.2:** (a) First step in creating the grid. Corner points are moved to desired location.  
(b) The final grid where the border of the grid are aligned with the polygon

## 5.2 Bed level approximation

The bed level approximation is divided in two parts: everything outside of the transition zone and everything inside it. Outside the transition zone, the physics based model as developed by Zervakis (2015), and shown in Section 2.1.1, can be applied. Outside the transition zone, the river is assumed to be in an equilibrium state which is not influenced by the bifurcation. The secondary flow ( $v$ ) in Eq. 2.5 is assumed to be zero. This is assumed because this flow is often much smaller than the primary flow. Also this flow is much harder to determine or derive, especially when data is scarce (Kalkwijk and Vriend, 1980),(Papanicolaou et al., 2007).

The physics based model requires several input parameters. The methods to obtain some of these parameters will be explained here. The parameter not discussed here do not require any calculations. The Chézy coefficient is derived from the Manning's roughness coefficient. According to Benson and Dalrymple (1984) the Manning's coefficient of a channel with bed material consisting of gravel with diameter of 2-64 mm is between 0.028 and 0.35. Based on the medium grain size in the river, the Manning's coefficient is determined. By using Eq. 5.4 the Manning's coefficient is converted to the Chézy coefficient. Herein is the equilibrium water depth used instead of the hydraulic radius ( $R$ ). This is justified because the river is much wider than deep. Since herein the Chézy coefficient is used as well, the values for both parameters are computed iteratively.

$$C = \frac{1}{n} R^{1/6} \quad (5.4)$$

The calibration coefficient, Eq. 2.3, is computed with Eq. 5.5 (Crosato, 2008). This parameter should be calibrated using available data. Since calibration is not possible for the rapid assessment tool, this empirical relation is used.

$$a = 0.1 \left( \frac{h_e}{D_{50}} \right)^{0.3} \quad (5.5)$$

where:

$h_e$  = Equilibrium water depth [m]

$D_{50}$  = median sediment grain diameter [m]

The curvature of the upstream river is calculated with Eq. 5.6. The average curvature of the entire upstream bend is used.

$$\gamma = \frac{B}{R_c} \quad (5.6)$$

where:

$B$  = upstream river width [m]

$R_c$  = Radius of the bend [m]

The physics based model, from Zervakis (2015), calculates the water depth of a given cross-section. In most cases the bed level is of more interest. The bed level is computed by adding the downstream water level and the extra height due to the slope of the area, to the calculated water depth.

The start and end of the transition zone is determined by the river width and the curvature of the upstream river. The upstream length is calculated with Eq. 4.1, this equation follows from the relation between upstream river width and upstream transition zone length, as found in Ch. 4.2.3, and the relation between upstream river curvature and upstream transition zone length, as found in Ch. 4.2.4

In Section 4.2.3 the relation between river width and downstream transition zone is found. For this study it is chosen to base the downstream transition zone length on the downstream river width. This is done because this makes it possible for downstream branches to have different transition zone lengths. The downstream transition zone is calculated with Eq. 4.2

## **5.3 Interpolation methods**

Four interpolation methods, to interpolate the bed level between the beginning and end of the transition zone, have been implemented. These are a single step method, linear interpolation, interpolation based on the Gaussian error function and, linear interpolation including bars and pools.

### **5.3.1 Single step method**

The single step method is the most basic method to model the transition from a single upstream branch to two downstream branches. With this method there is no transition zone. The input values for discharge, slope and width of branch 0 are used to compute the bed profile up to the bifurcation point. Downstream of the bifurcation point the values of branches 1 or 2 are used.

### **5.3.2 Linear interpolation**

With this method there is an transition zone. It starts and ends according to the relationship described in 5.2. The bed level in the transition zone is determined by linear interpolation between the bed level at the beginning and end of the transition zone.

### **5.3.3 Gaussian error function interpolation**

The third interpolation method is based on the Gaussian error function. This function is chosen to get a more smooth and natural transition between the begin and end of the transition zone. The Gaussian error function is defined as Eq. 5.7 (Andrews, 1998). The shape of the standard Gaussian error function is shown in Figure 5.3. The Gaussian error function is fit by applying it as in Eq. 5.8. In case the computed bed level at the begin and end of the

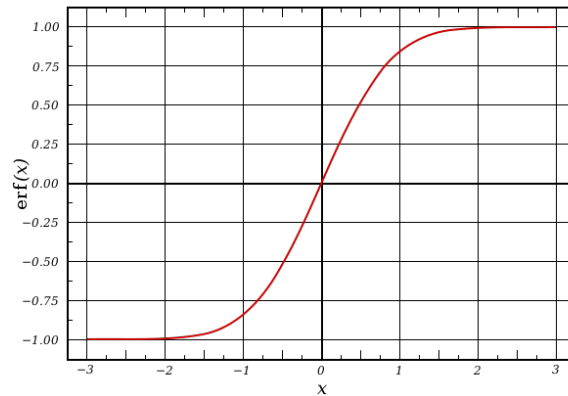


**Figure 5.3:** Standard Gaussian error function

transition zone are not equal to the computed bed levels for outside of the transition zone, the parameter  $c$  is reduced till the fit is good.

$$erf(x) = \frac{1}{\sqrt{\pi}} \int_{-x}^x e^{-t^2} dt \quad (5.7)$$

$$Bedlevel(x) = a * erf\left(\frac{x - b}{c * \sqrt{2}}\right) + d \quad (5.8)$$

where:

$a$  = Amplitude: ( $\text{abs}(\text{Bed level [TZ end]} - \text{Bed level [TZ begin]})$ ) [m]

$b$  = Location shift:  $((\text{TZ end} + \text{TZ begin})/2)$  [m]

$c$  = Slope:  $(\text{TZ end} - \text{TZ begin}) * (\text{Bed level [TZ end]} - \text{Bed level [TZ begin]})$

$d$  = Bed level shift:  $((\text{Bed level [TZ end]} - \text{Bed level [TZ begin]})/2)$  [m]

### 5.3.4 Linear interpolation with bars and pools

The linear interpolation method is extended, in order to account for bars and pools in the transition zone. The linear interpolation method is used because it is similar to the schematization used for the analysis of the water depth in Ch. 4 and described in Ch. 3.1.2. The Gaussian error function interpolation is not extended to account for bars and pools because it would be more difficult to find a good fit for this function. Also, since the size of the bars and pools are small compared to the length, the error function will lead to a similar profile as the linear method will.

From the analysis it follows that the length of the bars or pools is related to the length of the transition zone. The length of the upstream bars or pools is described with Eq. 4.3, the length of the downstream bars or pools is described with Eq. 4.4. The size of the bars and pools is related to the width of the upstream river, this is described with Eq. 4.5 and 4.6. The size is equal for up and downstream bars or pools.

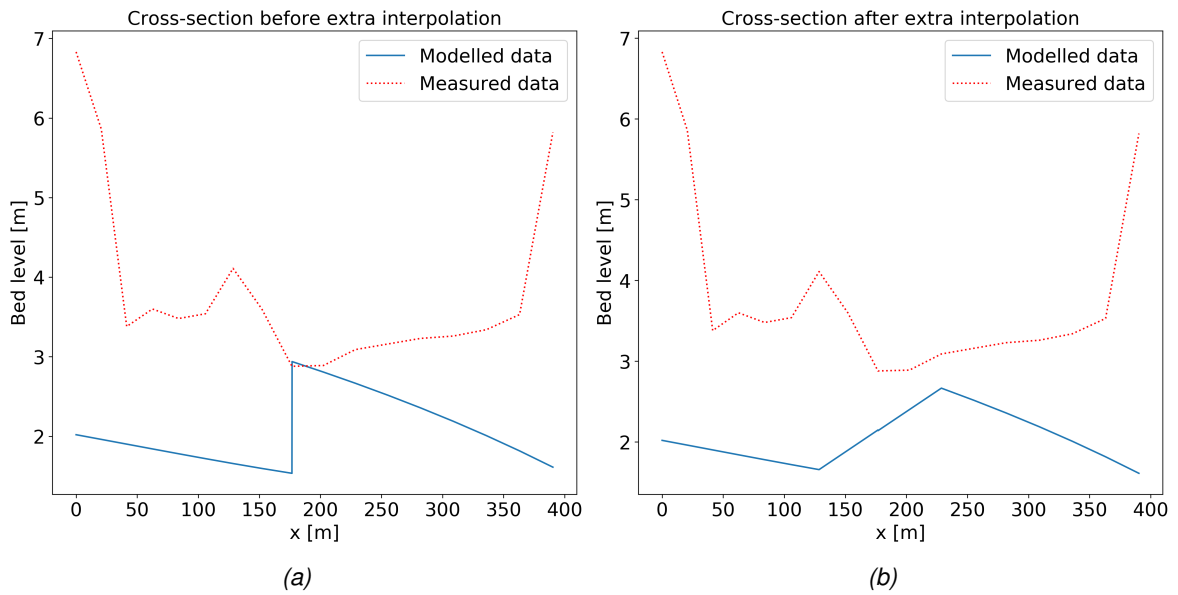


**Figure 5.4:** Cross-sectional profile upstream of bifurcation point. (a) before cross-sectional interpolation (b) after cross-sectional interpolation

## 5.4 Cross-sectional profiles

Due to the way the grid is created and the interpolation between upstream and downstream, an error occurs in centre of the upstream part of the transition zone. An unnatural division occurs in the middle, see Figure 5.4a. To prevent this, the bed level in the centre of the cross-sectional profile is computed based on linear interpolation in the cross-sectional profile. The bed level of the four lines in the centre of the grid are computed this way. The interpolation is between the bed level left and right of this. This results in a cross-sectional profile as in Figure 5.4b



# Results

In this chapter the results will be presented from the application of the extended rapid assessment tool on three study cases. A global description of the bifurcation will be given, any anomalies that occur in the bed level will be mentioned. The results are divided into two parts per study case. The first is where the upstream and downstream bed levels are calculated by using the physics based model. The other is where the measured bed level is used for the upstream and downstream river sections.

## 6.1 Study cases

The extended tool has been applied on three bifurcations. Two of those are in the Rhine and one in the Danube. These are shown in Fig. 6.1. The first one is in the Rhine delta at the Pannerdensche Kop, the second one is also in the Rhine delta at the IJssel Kop and the third is in the Danube. High accuracy bed level data is available for these bifurcations. The bed level data for the Rhine is provided by Rijkswaterstaat and are available from measurements in May 2017. The data for the Danube has been gathered by Deltares in 2013. The grid that is used consists of 250 by 18 cells. Multibeam echo sounding is used to gather this data. This method results in a very low error. Ernstsens et al. (2006) analysed measurements of the Danish Waddensea where Multibeam echo sounding was used, here an error of  $\pm 2cm$  was found for one survey and  $\pm 8cm$  for another. Jantti (1989) analysed the results from a survey in the Atlantic Ocean. Here the standard deviation on the error map was less than 1%.



**Figure 6.1:** The three bifurcations of the study cases. From left to right: Pannerdensche Kop, IJssel Kop and Danube - Bala bifurcation

### 6.1.1 Pannerdensche Kop

Ten kilometres from where the Rhine enters the Netherlands, it bifurcates into the Waal and Pannerdensch Kanaal. The bifurcation is shown in Figure 6.2. Two thirds of the discharge from the Bovenrijn flows into the Waal the other thirds into the Pannerdensch Kanaal (Rijkswaterstaat, 2018b). The curvature the Bovenrijn upstream of the bifurcation is 0.037. In Figure 6.3 is the measured bed level of the Pannerdensche Kop shown. There is a large bed level difference between the right side of the Bovenrijn and the Pannerdensch Kanaal, around 2.5 m in the centre of the canal. The difference in equilibrium water depth of the Bovenrijn and the Waal, computed with Eq. 2.2, is only 0.08 m.

Groynes are present at both sides of the Rhine, in the Waal and Pannerdensch Kanaal they are only at the right bank. A small analysis of the direct effect of groynes on the bed level is performed. This analysis can be seen in Appendix C. The conclusion of this analysis is that the effect of groynes is of a much smaller order than the effect of the bifurcation on the bed level.

The used parameters for the physics based model are shown in Table 6.1. The slope is derived from the change in water level as described in van der Veen and van der Veen (2010). The median sediment grain diameter is derived from documents provided by Rijkswaterstaat

River branch	Q	W	$h_e$	C	i	$D_{50}$	a
Bovenrijn	2000	350	6.43	45.5	$5.95 * 10^{-5}$	$3.00 * 10^{-3}$	1.00
Waal	1333	230	6.04	45.0	$1.00 * 10^{-4}$	$1.75 * 10^{-3}$	1.15
Pannerdensch Kanaal	667	130	6.35	45.4	$4.89 * 10^{-5}$	$5.00 * 10^{-3}$	0.85

**Table 6.1:** Parameters for the Pannerdensche Kop

**Transition zone** The transition zone is computed with Eq. 4.1 and 4.2 as well as derived from the measured data by using the method described in Ch. 3.3.1. The computed upstream transition zone length is 603 m. This is larger than the upstream transition zone length based on the measured data, which is 373 m.

The calculated downstream transition zone is 629 m for the Waal and 408 m for the Pannerdensch Kanaal. The measured data shows a downstream transition zone of respectively 885 m and 0 m. The non existence of the downstream transition zone in the Pannerdensch Kanaal an interesting phenomena which can not be explained by the results form the bifurcation analysis. The fact that the Pannerdensche Kanaal is a canal instead of a natural river might affect the downstream transition zone.

### Results - physics based model

In Figure 6.4 the modelled bed level is shown, using the single step interpolation, together with the error map. Figures for the other interpolation methods can be found in Appendix D. The RMSE is computed for six zones around the bifurcation. These zones are: The whole

transition zone (TZ all), the right side of the upstream transition zone and downstream transition zone in branch 1 (TZ 1), the left side of the upstream transition zone and downstream transition zone in branch 2 (TZ 2), the part upstream of the transition zone (Upstream), the part in branch 1 downstream of the transition zone (Downstream branch 1) and the part in branch 2 downstream of the transition zone (Downstream branch 2). The RMSE can be seen in Table 6.2.

There are no major variations between the errors in all zones. The error in the transition zone is larger than outside the transition zone. The main reason for the error can be found at the sides of the rivers. The model does not take river banks in account in this case. The polygon of the river is chosen such that the banks are almost not in it either. However, some parts of the banks or groynes are still in it. Especially around the bifurcation point this leads to a considerable error. In the Pannerdensche Kanaal, the physics based model computes a bed level that is higher than the measured bed level. This leads to a large RMSE and this has an effect on the RMSE in the right side of the transition zone (TZ 1). Overall the measured bed level is higher than the modelled bed level.

### Results - measured data

In Table 6.3 are the RMSE shown for the four interpolation methods when the measured data is used in the areas outside the transition zone. In this case there is no error outside the transition zone, these is therefore not shown in the table. In Appendix D are the modelled bed level and the error map shown for all interpolation methods. When using the measured data as basis for the interpolation, the RMSE is not the same for all four methods. The single step method has the highest RMSE. This is mainly caused by the error at the right side of the transition zone (TZ 1).



**Figure 6.2:** Pannerdensche Kop

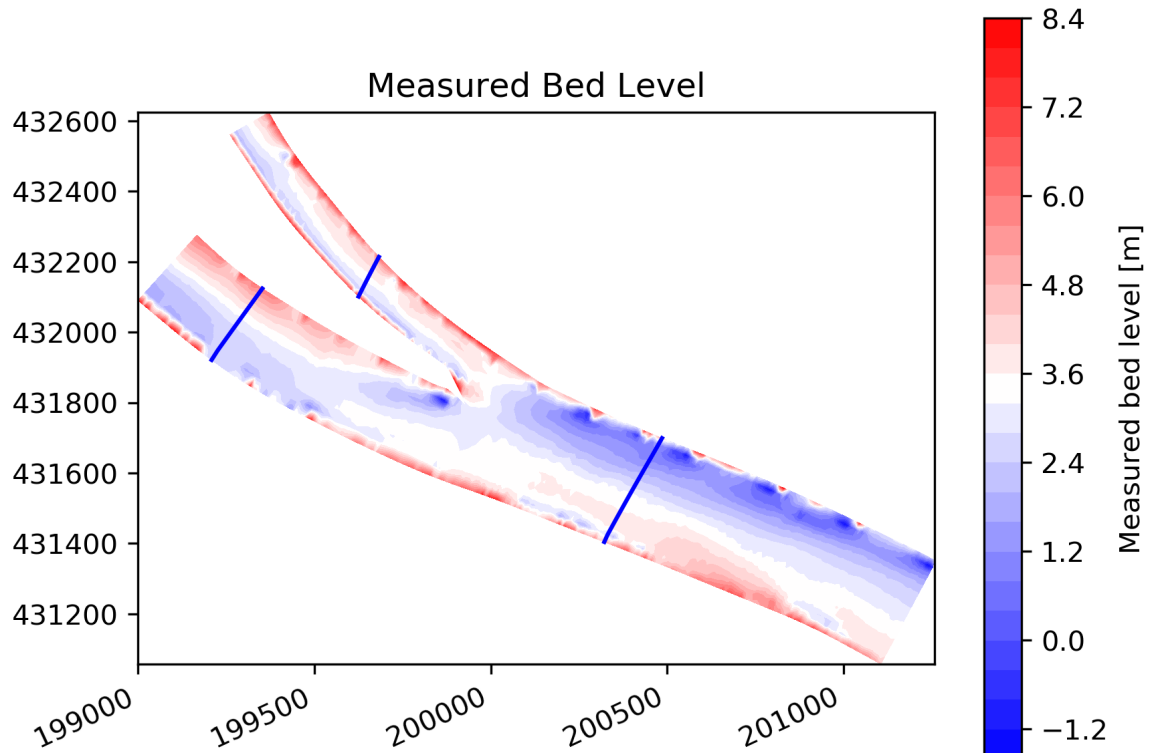


**Figure 6.3:** Measured bed level at the Pannerdensche Kop

RMSE [m]	Zone					
	TZ all	TZ 1	TZ 2	Bovenrijn	Pannerdensch Kanaal	Waal
Single step	1.78	1.92	1.67	1.57	2.48	1.75
Linear	1.72	1.90	1.57	1.57	2.48	1.75
Error func	1.73	1.90	1.60	1.57	2.48	1.75
Linear-Bar Pool	1.64	1.78	1.51	1.57	2.48	1.75

**Table 6.2:** RMSE for the bed level per zone and interpolation method around the Pannerdensche Kop bifurcation

RMSE [m]	Zone		
	TZ all	TZ 1	TZ 2
Single step	1.01	1.08	0.95
Linear	0.80	0.80	0.80
Error func	0.79	0.75	0.80
Linear - Bar Pool	0.89	0.80	0.95

**Table 6.3:** RMSE for the bed level per zone and interpolation method around the Pannerdensche Kop bifurcation

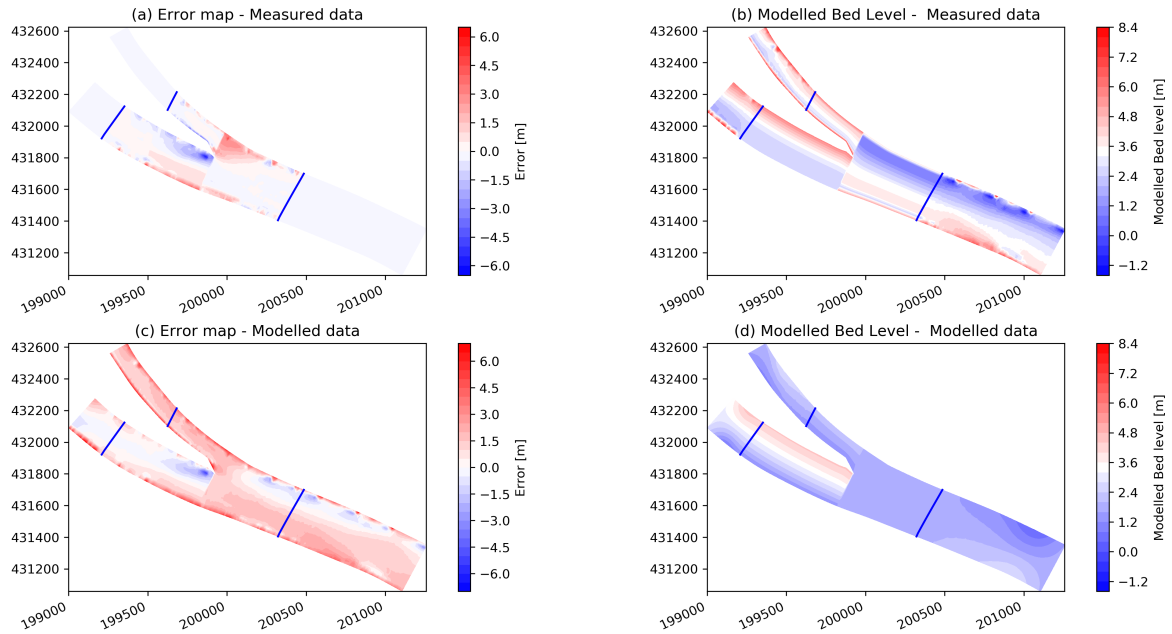


**Figure 6.4:** (a) The error map and (b) the modelled bed level, based on the physics based model at the Pannerdensche Kop. (c) The error map and (d) the modelled bed level, based on measured data. The blue lines indicate the begin and end of the transition zone

### 6.1.2 IJssel Kop

Eleven kilometres from where the Rhine bifurcates into the Waal and Pannerdensch Kanaal, the Pannerdensch Kanaal bifurcates into the Nederrijn and the IJssel. Here the discharge distribution is similar to the Pannerdensche Kop bifurcation. Two thirds of the discharge flow into the Nederrijn and one third into the IJssel (Rijkswaterstaat, 2018b). In Figure 6.5 the bifurcation of Pannerdensch Kanaal into the Nederrijn en IJssel is shown. In Figure 6.6 is the bed level at the IJssel Kop shown. Interestingly, the IJssel appears to be much deeper than the Nederrijn. The equilibrium water depth of the IJssel is only 3.72 m, where that of the Nederrijn is 7.33 m. The IJssel has a deep pool just downstream of the bifurcation. The Nederrijn only has a few deeper pools where groynes are present.

The used parameters for the physics based model are shown in Table 6.4. The slope is derived from the change in water level as described in van der Veen and van der Veen (2010). The median sediment grain diameter is derived from documents provided by Rijkswaterstaat. The curvature upstream of the bifurcation is here 0.065.

River branch	Q	W	$h_e$	C	$i$	$D_{50}$	$a$
Pannerdensch Kanaal	666	130	6.35	45.4	$4.89 * 10^{-5}$	$5.00 * 10^{-3}$	0.85
Nederrijn	444	100	7.33	46.5	$2.28 * 10^{-5}$	$2.00 * 10^{-3}$	1.17
IJssel	222	70	3.72	41.5	$1.12 * 10^{-4}$	$6.00 * 10^{-3}$	0.69

**Table 6.4:** Parameters for the IJssel Kop

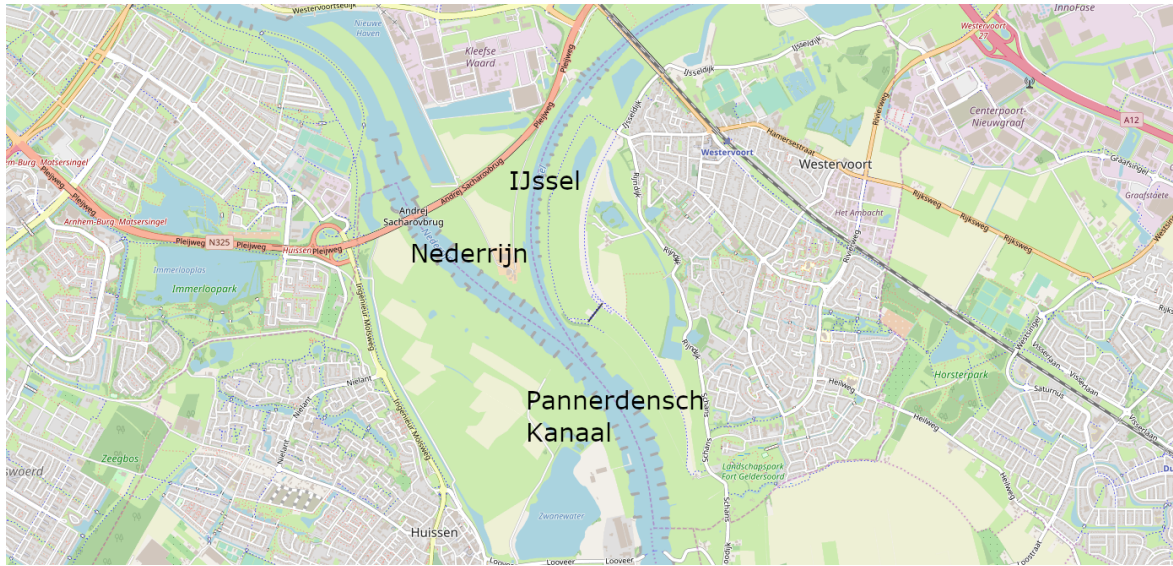


Figure 6.5: IJssel Kop

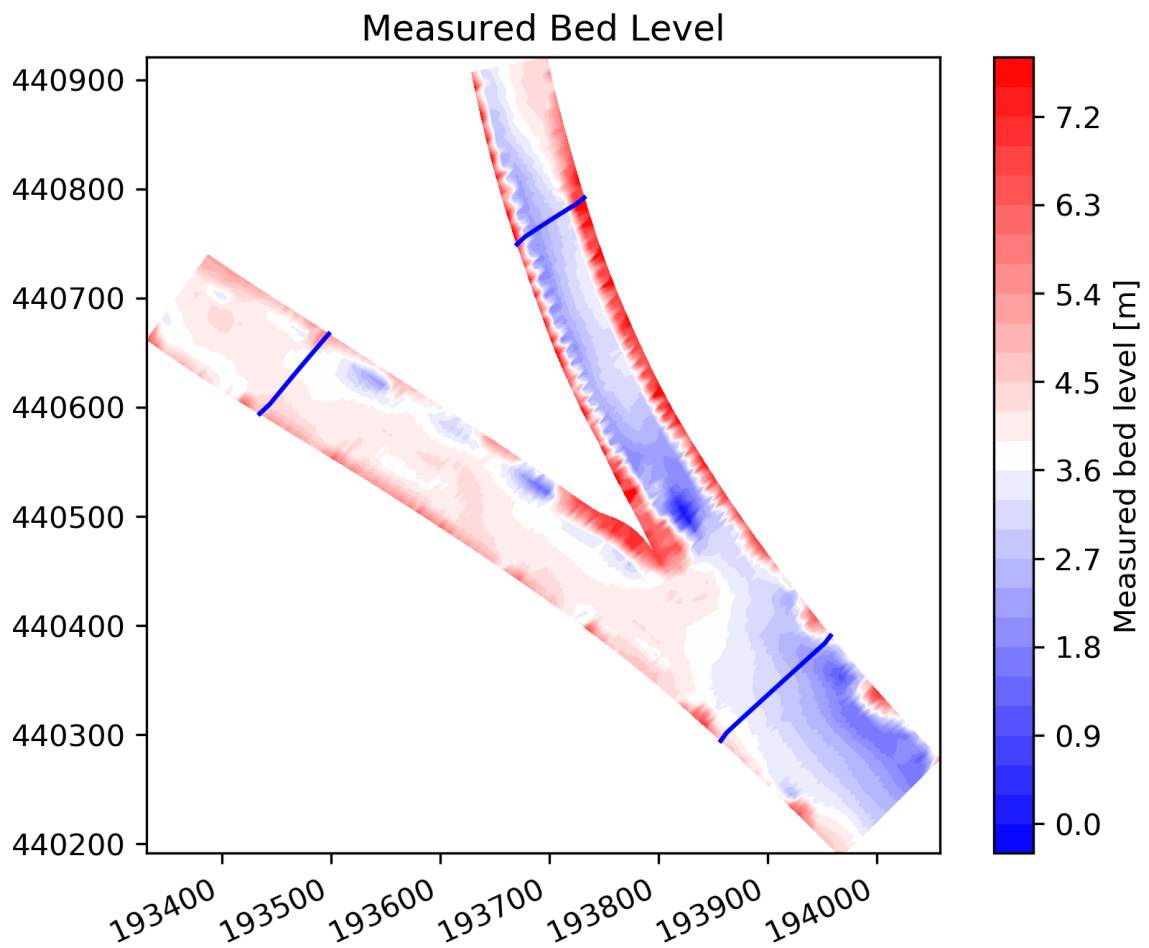


Figure 6.6: Measured bed level at the IJssel Kop

**Transition zone** The transition zone is computed with Eq. 4.1 and 4.2 as well as derived from the measured data by using the method described in Ch. 3.3.1. The computed upstream transition zone length is 190 m. This is smaller than the upstream transition zone length based on the measured data, which is 287 m on average but varies over the width of the river. On the left side the upstream transition zone is 244 m and on the right side it is 330 m. The curvature of the upstream river can have caused this difference. The much smaller computed transition zone length is might be due to the used constant in the equation. The -494 constant decreases the transition zone significantly when the river width and curvature are both small.

The calculated downstream transition zone is 342 m for the Waal and 275 m for the Pannerdensch Kanaal. The measured data shows a downstream transition zone of respectively 130 m and 488 m. The error between calculated and measured downstream transition zone is considerably, around a factor two.

### Results - Physics based model

In Figure 6.7 is the modelled bed level, using the linear interpolation method, together with the error map shown. The bed level outside the transition zone is calculated with the physics based model. The RMSE is computed for the same six zones around the bifurcation as before. These can be seen in Table 6.5. In Appendix D are the modelled bed level and the error map shown for all interpolation methods.

The bed level of the Nederrijn is a lot lower than the bed level in the IJssel according to the model. The measured data shows that the opposite is true. This leads to large errors in this part of the river, especially in the Nederrijn. The Pannerdensch Kanaal has a much lower error. This has an effect on the error in the transition zone. The error in the Nederrijn side is higher than in the IJssel side. The linear interpolation has an error that is much lower for the IJssel side (TZ 1) than the other interpolation methods have. For all other zones the error is about equal for all interpolation methods. Some groynes are still present in the measured bed level and around the bifurcation point, some parts of the banks are present. This leads to some local large errors. Using a smaller polygon would lead to different errors. The river would appear smaller than it actually is, this would lead to a lower bed level in the physics based model.

RMSE [m]	Zone					
	TZ all	TZ 1	TZ 2	Pannerdensch Kanaal	IJssel	Nederrijn
Single step	2.34	2.00	2.60	0.92	1.83	3.12
Linear	2.06	1.70	2.34	0.92	1.83	3.12
Error func	2.13	1.81	2.38	0.92	1.83	3.12
Linear - Bar Pool	2.07	1.81	2.28	0.92	1.83	3.12

**Table 6.5:** RMSE for the bed level per zone and interpolation method around the IJssel Kop bifurcation

## Results - measured data

In Table 6.6 are the RMSE shown for the four interpolation methods when the measured data is used in the areas outside the transition zone. In Figure 6.7 is the modelled bed level and error map shown. In Appendix D are the modelled bed level and the error map shown for all interpolation methods. Now some difference in RMSE between the interpolation methods are present. The linear interpolation that includes bars and pools has the lowest RMSE. The difference is mainly caused by the error at the right side of the transition zone (TZ 1). Here are the difference the largest as well. The pool in the IJssel will be determining factor for the RMSE in this zone.

RMSE [m]	Zone		
	TZ all	TZ 1	TZ 2
Single step	1.09	1.44	0.65
Linear	0.99	1.25	0.68
Error func	1.03	1.30	0.70
Linear - Bar Pool	0.92	1.15	0.65

**Table 6.6:** RMSE for the bed level per zone and interpolation method around the IJssel Kop bifurcation

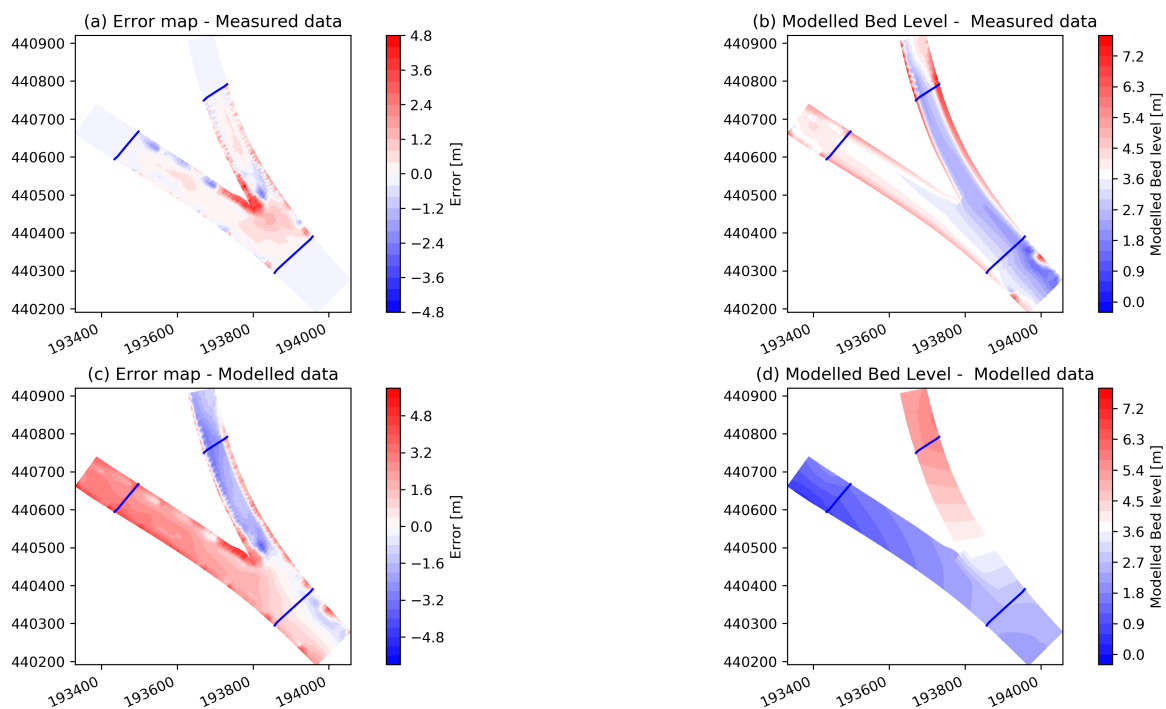


**Figure 6.7:** (a) The error map and (b) the modelled bed level, based on the physics based model at the IJssel Kop. (c) The error map and (d) the modelled bed level, based on measured data. The linear interpolation method is used. The blue lines indicate the begin and end of the transition zone

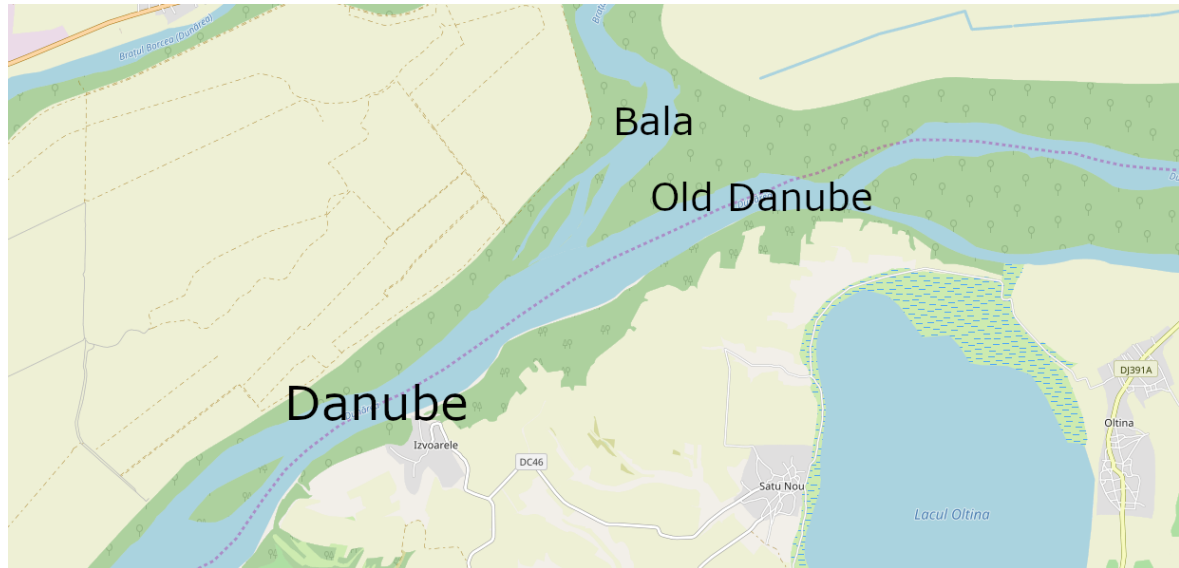


**Figure 6.8:** Bifurcation in the Danube

### 6.1.3 Danube - Bala

In Figure 6.8 a bifurcation is shown that is located 20 km east of Călărași, Romania. Here bifurcates the Danube into the old Danube and Bala. Bala has been artificially narrowed, the width is only 200 m here. In Figure 6.9, the measured bed level is shown. At 1700 m upstream of the bifurcation there is a rock formation in the right river bank. This causes a disruption in the bed level around this point. The bed level becomes much deeper than normal. Around 60% of the discharge from the Danube flows into the Bala, the rest into the Old Danube. The used parameters for the physics based model are shown in Table 6.7. The slope,  $D_{50}$  and discharge are described in Yossef (2013). The slope,  $D_{50}$ , and downstream water level are not described for all three branches. The downstream water level is given just upstream of the bifurcation. Based on the given slope and distance between the beginning and end of the transition zone, the downstream water levels are calculated. According to Crosato (2008) the calibration coefficient should be between 0.4 and 1.2. The calculated  $a$  is almost twice as high for all three branches. This would lead to an overestimation of the effect of the curvature on the bed level. Instead of using the calculated value of  $a$ , the value of 1.2 is used for all three branches. The upstream curvature of the Danube is 0.025.

River branch	Q	W	$h_e$	C	i	$D_{50}$	$a$
Danube	7000	645	10.64	49.4	$4.00 \cdot 10^{-5}$	$2.69 \cdot 10^{-4}$	2.39
Bala	4263	300	12.53	50.8	$4.00 \cdot 10^{-5}$	$2.69 \cdot 10^{-4}$	2.51
Old Danube	2737	515	6.93	46.0	$4.00 \cdot 10^{-4}$	$2.69 \cdot 10^{-4}$	2.11

**Table 6.7:** Parameters for the Danube

**Transition zone** From this curvature and the width it follows that the upstream transition zone is 1290 m. The transition zone according to the measurements is 875 m at the left

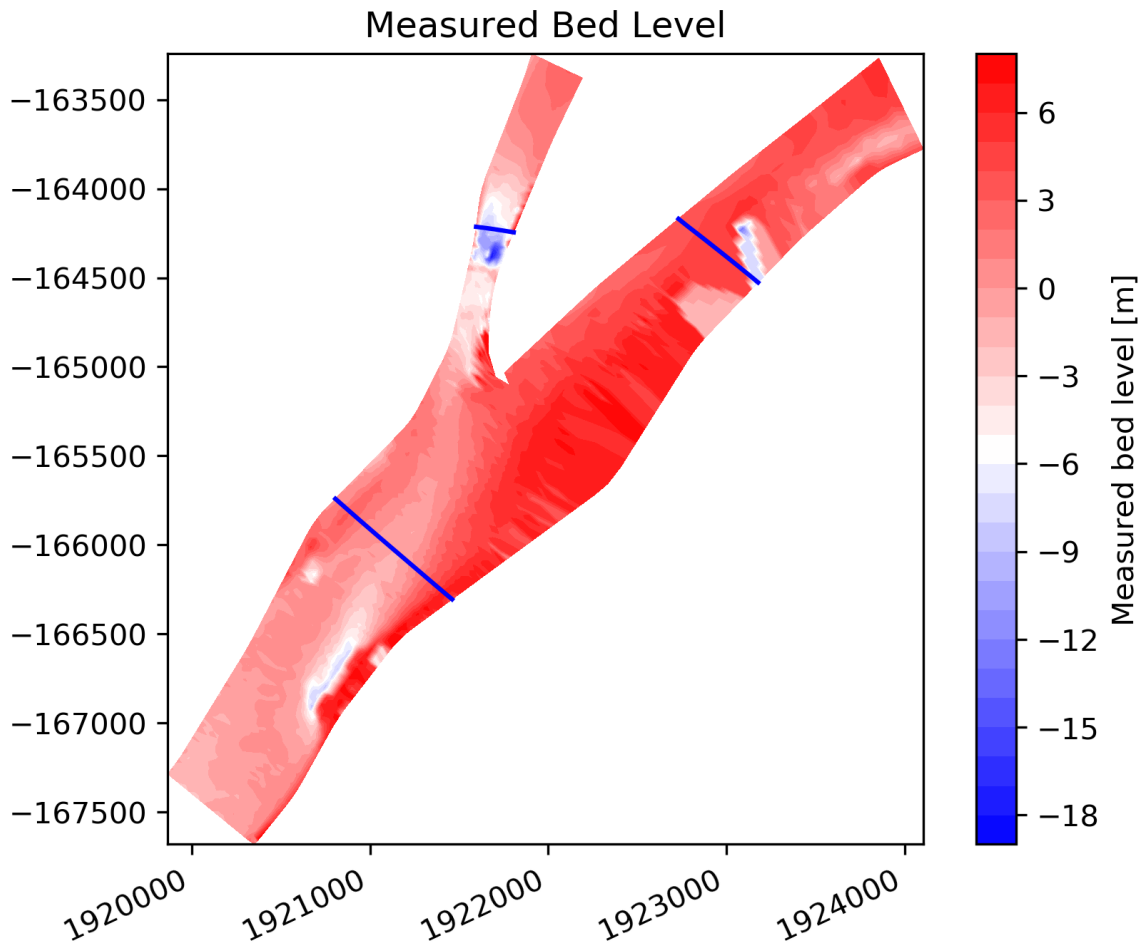


**Figure 6.9:** Measured bed level at the Danube - Bala bifurcation

side of the river and 1586 m at the right side. The calculated transition zone is close to the average measured transition zone. The difference in transition zone between the left and right side of the river are caused by the upstream rock formation. The large pool connects seamlessly with the the bed level of the Old Danube. This makes it seem that the transition zone starts at the deepest part of the pool, where it in fact start later.

The computed downstream transition zones are 781 m in the Bala and 1259 m in the Old Danube. The transition zone derived from the measured data is very different. The downstream transition zone in the Bala is only 601 m and in the Old Danube is 0 m. Especially the Old Danube has a big difference between measured and computed transition zone length. This difference, or the fact that the downstream transition zone is 0 m, cannot be explained by the results from the bifurcation analysis. The discharge distribution is shifting more in favour of Bala in the last few years (Yossef, 2013), this shift will have an influence on the bed level and might explain the downstream transition zone.

RMSE [m]	Zone	TZ all	TZ 1	TZ 2	Danube	Old Danube	Bala
	Single step		4.64	3.54	5.74	5.24	4.58
Linear		4.28	3.33	5.24	5.24	4.58	2.84
Error func		4.39	3.42	5.38	5.24	4.58	2.84
Linear–Bar Pool		4.43	3.373	5.49	5.24	4.58	2.84

**Table 6.8:** RMSE for the bed level per zone and interpolation method around the Danube - Bala bifurcation

### Results - Physics based model

In Figure 6.10 is the modelled bed level, using Gaussian error function interpolation method, together with the error map shown. In the modelled bed level a local depth can be seen just upstream of the transition zone. This depth is caused by the curvature in the grid. The high calibration coefficient causes a high slope in the cross-sectional bed level profiles when the river has a curvature. This error is seen back in the RMSE of the upstream part in Table 6.8. In Appendix D are the modelled bed level and the error map shown for all interpolation methods.

The linear interpolation gives the lowest RMSE, the linear interpolation including bars and pool and the Gaussian error function interpolation give slightly better results than the single step interpolation. The man made deep pool in the Bala branch is not accurately modelled.

### Results - measured data

In Table 6.9 are the RMSE shown for the four interpolation methods when the measured data is used in the areas outside the transition zone. In Appendix D are the modelled bed level and the error map shown for all interpolation methods. The Gaussian error function interpolation gives a higher error in zone 2 than the single step method gives. This is the only case where the single step method does not give the highest RMSE. Again the linear interpolation gives the lowest RMSE. The error is at the right side of the transition zone (TZ 1) is determining for the change in RMSE. The linear interpolation achieves a significant lower RMSE than the other methods. The deeper zone in the Bala is much better modelled now. In the Old Danube is also a pool visible just downstream of the transition zone. This leads to a lower bed level at the right side of the Old Danube through the whole downstream transition zone.

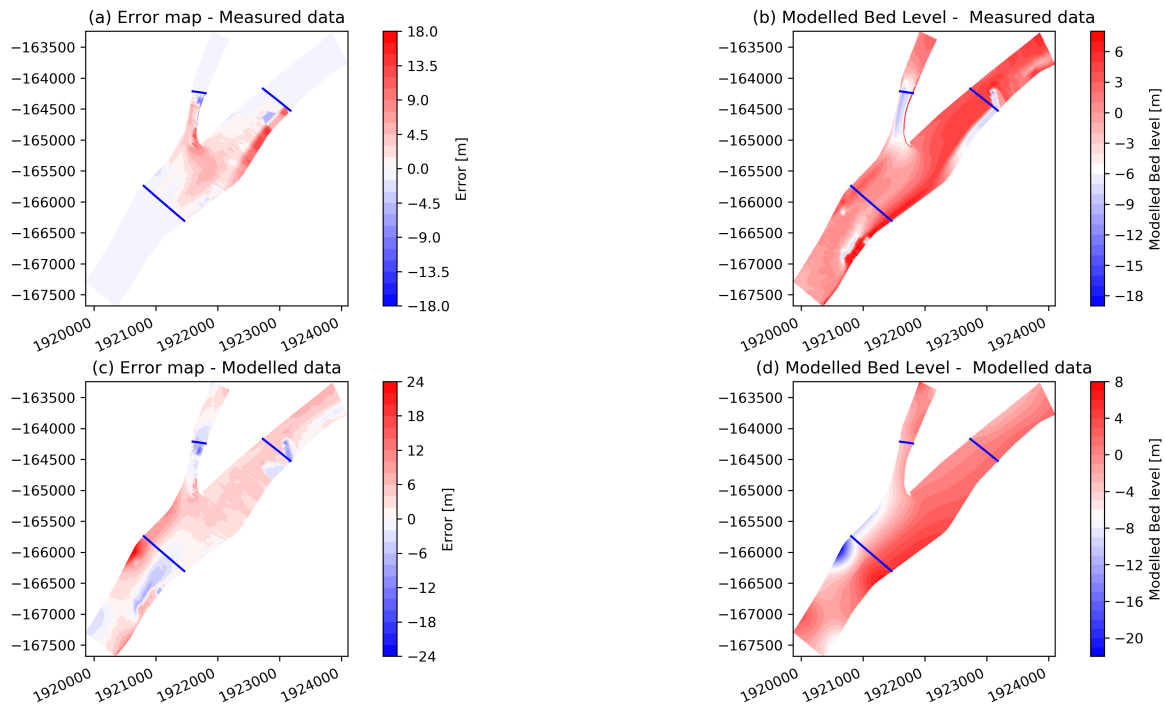


**Figure 6.10:** (a) The error map and (b) the modelled bed level, based on the physics based model at the Danube - Bala bifurcation. (c) The error map and (d) the modelled bed level, based on measured data. Gaussian error function interpolation method is used for these figures. The blue lines indicate the begin and end of the transition zone

RMSE [m]	Zone		
	TZ all	TZ 1	TZ 2
Single step	4.37	4.68	3.92
Linear	3.76	3.79	3.73
Error func	4.15	4.26	4.00
Linear-Bar Pool	4.01	4.30	3.62

**Table 6.9:** RMSE for the bed level per zone and interpolation method around the Danube - Bala bifurcation

## 6.2 Sensitivity analysis

A sensitivity analysis to the accuracy of the extended rapid assessment tool is performed. This sensitivity analysis is done based on the Pannerdensche Kop case study. The sensitivity of the RMSE to the upstream river curvature, upstream river width and the downstream river width is analysed. The parameters have been varied between 0.6 and 1.4 times the original value. The linear interpolation method is used for this sensitivity analysis. The measured data is used outside the transition zone.

The transition zone length is equally sensitive to all three parameters, since all have a linear relationship with the transition zone length. For the Pannerdensche Kop, the upstream river width will be parameter that has the most influence on the transition zone length. The total transition zone length is computed with:  $TZ_{length} = 2.55 * W_{upstream} + 5468 * \gamma + 2.21 * W_{downstream} - 373 = 943.5 + 204.8 + 508.3 - 373 = 12.83.6 m$

In Figure 6.11a, the relative RMSE for the whole transition zone around the Pannerdensche Kop is shown. Here the RMSE seems insensitive to a change in any of the parameters. Only when the upstream river width is around 0.7 times the original width, the RMSE increases significantly. When only the RMSE of the centre of the branches is taken into account (Figure 6.11b), the graph gives a different impression. The RMSE now seems sensitive to both upstream and downstream river width and not very much to river curvature.

However, this sensitivity analysis can give a wrong impression of the sensitivity. This has three reasons. Firstly, is the use of the measured data outside the transition zone. By changing the parameters, the transition zone start or end changes. If the computed start and end of the transition zone would exactly match the actual transition zone and then the computed transition zone would be made smaller, the RMSE would not change much since both the total error as well as the number of samples decreases.

The second reason is that the begin and end of the transition zone are computed separately. A change in upstream river width and upstream river curvature changes the begin location of the transition zone. A change in downstream river width changes the end of the transition zone. Since the three parameters are varied separately, there will always be an error in the location of the transition zone. This can lead to two different computed bed levels with the same RMSE (Figure 6.12).

The third reason is the error that occurs at the river banks. Here the bed level is not determined by the bifurcation. The bed level here is irregular and this leads to errors that are independent of the location of the transition zone. This causes Figure 6.11a to be more spread out compared with Figure 6.11b.

A better way to perform a sensitivity analysis would be by using the physics based model outside the transition zone. For this the physics based model should be calibrated, in order to minimise the error there. This would solve the first mentioned reason. The second problem could be solved by setting only looking at the error in the upstream transition zone when varying the upstream river width and the upstream curvature, and only looking at the error in the downstream transition zone when varying the downstream river width.

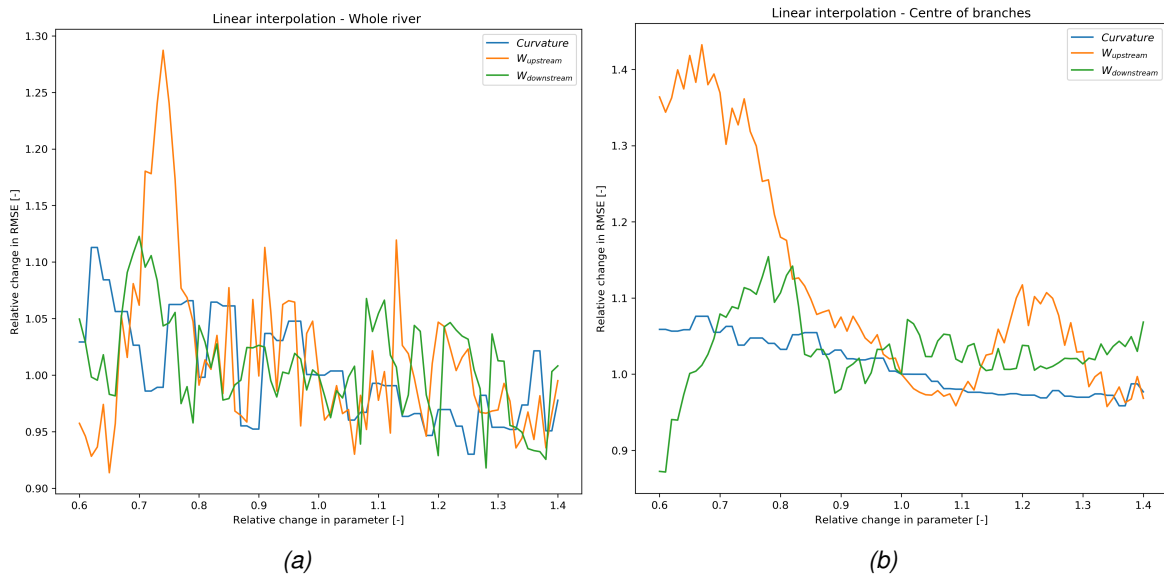


**Figure 6.11:** Sensitivity analysis (a) RMSE for the whole transition zone (b) RMSE for the centre of the branches.

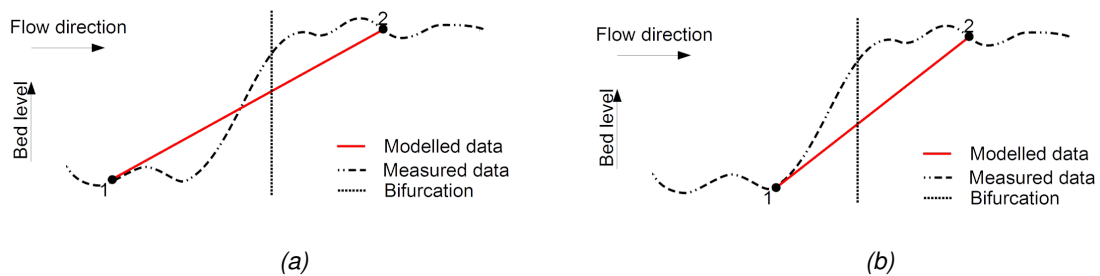


**Figure 6.12:** Different bed levels with possibly the same RMSE

## 6.3 Summary

The calculated transition zone length differs significantly from the actual transition zone. In some cases the calculated zone is much too large, in others too small. Estimating the upstream transition zone length based on only upstream river width and curvature gives a reasonably good estimation. However the start of the transition zone can differ over the width of the river. This can be seen in at the IJssel Kop and the Bala bifurcation. The downstream transition zone length is difficult to predict as well. Only for the Waal and Bala branch is the modelled length close to the computed one. For all other branches it is off by a factor two or more.

When using the physics based model to calculate the bed level upstream and downstream of the transition zone, the different interpolation methods do not lead to very different results. In general the error in the transition zone is similar to the error outside the transition zone. Linear interpolation leads to the lowest RMSE in two of the three study cases. The addition of bars and pools does in one case increase the accuracy and in one it does not. In the IJssel case study, they have the same RMSE. In all case studies the RMSE decreases when another interpolation method than the single step method is used.

When using the measured bed level upstream and downstream of the transition zone, the interpolation methods do have varying accuracies. The single step interpolation method performs the least well. The linear interpolation gives the lowest RMSE in two case studies. The addition of bars and pools does increase the accuracy in the IJssel case study, in the other two case studies the RMSE is lower than for only linear interpolation.



# Discussion

The results from the bifurcation analysis and the implementation and application of the extended rapid assessment tool will be discussed in this chapter. Three topics will be discussed. The bifurcation analysis, the performance of the extended rapid assessment tool and, the study cases.

## 7.1 Bifurcation analysis

The modelled data used for the bifurcation analysis may have influenced the outcome of the analyses as performed in this study. This may have happened in two ways. Firstly, by the accuracy of the numerical model and secondly, by identifying relationships that are case specific. This will be discussed in this section.

### **Numerical model**

The bed level data can be an inaccurate representation of a bifurcation. However, since the physics governing the hydrodynamics and morphodynamics in the model used are well implemented and validated, the generated bed level will be similar to data coming from a scale study. These data will still not be the same as measured data from actual river bifurcations. The fixing of river banks will not occur in real alluvial rivers. This affects the topography of the river: an increase of discharge in a branch is directly linked to an increase in water depth. In a real river the width of a river may increase as well when the discharge increases. The fixing of the banks will lead to more extreme changes in bed level around the bifurcation. The analysis shows a weak relation between difference in water depth between the start and end of the transition zone. This could mean that the identified transition zones are influenced by the fixing of the banks. Especially, the relationship used for calculating the downstream transition zone, will be affected.

In some scenarios the location of the four points used in the schematization of the bed level, changes between two locations that are far apart in sequential time steps. This leads to a spreading in the found transition zone lengths. This weakens the found relationships in the bifurcation analysis. Reducing the step size used to find the optimal location of the

points in the schematization can help to prevent this behaviour.

## Relationships

The use of the data generated by the model may also have lead to identified relationships that are case specific. Parameters like the discharge and slope have been constant in all scenarios. These are important parameters for the flow velocity in the river, which is an important parameter for sediment transport. The sediment transport is determining the bed level in the river. Since these parameters have not been varied, the relationships identified may be specific for bifurcations with the used discharge and slope. The constant that are used in Eq. 4.1 and Eq. 4.2 may likely be specific for the analysed type of bifurcation.

The flow velocity has not been analysed in this study because it cannot be applied in the extended rapid assessment tool. However, this parameter does impact the way the bed level is shaped. Changes in flow velocity lead to erosion or deposition of sediment. The flow velocity is directly related to the water depth via:  $Q = h * W * v$ . This makes it hard to estimate the flow velocity when the water depth is unknown. This is per definition the case, when the extended rapid assessment tool is applied.

The found relation between upstream river width and upstream transition zone length is in agreement with the findings from (Pittaluga et al., 2003) who found it to be between two to three times the river width. From the analysis in Section 4.2.4 it follows that the curvature has an effect on the transition zone length as well. This is probably due to the increased transverse slope and the length required for the bed level to become more or less flat before the bifurcation.

The downstream transition zone length is also related to the river width. However, due to the set-up of the model in the study of Kleinhans et al. (2008), it could not be derived if the downstream or upstream river width is a better predictor for the downstream transition zone length. In the model set-up the downstream branches are exactly half the width of the upstream branch. The relationship that is found and used for the downstream transition zone is a weak one. More research on downstream transition zones is required to find stronger relationships.

In order to verify the applicability of the equations on different bifurcations, more research on the effect of different parameters is required. Parameters that could be analysed are the discharge, slope, different downstream river widths and flow velocity.

## 7.2 Performance of the extended rapid assessment tool

The performance of the extended rapid assessment tool is depending on the selected interpolation method as well as on the accuracy of the bed level data outside the transition zone. The use of the physics based model will be discussed here as well as the performance of the interpolation methods.

### 7.2.1 Physics based model

The interpolation methods all rely on the accuracy of the bed level that is computed for the areas outside the transition zone. The accuracy of the physics based model is dependent on several parameters. One of these parameters is the calibration coefficient. Eq. 5.5 gives an indication of the value for this parameter. However this value is only for use as an initial value for the calibration of the model. Since calibration is not possible when the extended rapid assessment tool is applied, this will stay a major cause for errors in the computed bed level. Accurate information about the  $D_{50}$  of a river can help to reduce the resulting error.

The error in the zones outside the transition zone can be as large as the difference in bed level up- and downstream of the zone. This makes it difficult to compare the interpolation methods, since the error in the transition zone can be determined by the physics based model instead of the used interpolation method. Calibrating the physics based model would help increasing the accuracy and thus the error in the transition zone would be more determined by the interpolation method that has been applied.

### 7.2.2 Interpolation methods

When the measured data is used outside the transition zone, instead of the values calculated by the rapid assessment tool, the four interpolation methods have significant differences in their accuracy. As expected, the single step interpolation method performs worst in almost all cases. Only in the left branch of the Danube, the Gaussian error function interpolation performs worse. This can be explained by a large pool, with its deepest point just at the end of the transition zone.

The linear interpolation method and linear interpolation including bars and pools perform best over all. When the bars and pools in the transition zone are correctly modelled, the accuracy of the extended rapid assessment tool increases. When this is not the case, only linear interpolation will be more accurate. The river width is probably an unsuitable predictor for the size of the bars and pools. Also, the downstream transition zone length is not correctly estimated yet. This causes the prediction of the bar and pool in the downstream zone to be off as well. Better understanding of the occurrence of bars and pools in the transition is required to predict when they and where those occur.

The Gaussian error function interpolation method does not perform better than the linear interpolation method. The Gaussian error function adds a gradually increasing or decreasing slope at the start and end of the transition zone. The slope in the middle of the transition zone is steeper than for the linear interpolation. The gradually changing slope at the begin and end of the transition zone might have little effect on the RMSE since the changes in bed level are small compared to the length of the transition zone. The steeper slope in the middle may have lead to an increase in the RMSE

## 7.3 Study cases

The error in the measured data is much smaller than the error between measured data and modelled data. The multibeam echo sounding method used to measure the data is a reliable method for measuring water depth. It can be assumed that the measurement error has no significant effect on the observed accuracy of the extended rapid assessment tool.

### 7.3.1 Pannerdensche Kop

The bed level at bifurcations is difficult to describe using the analysed parameters. The curvature does have an effect on the bed level at the bifurcation. The curvature of the upstream river leads to a transverse slope where the deeper side will be in the outer bend. When the branch opposite of the outer bend has a higher discharge than the branch at the outer bend side, the main flow will have to cross the river. This leads to deeper water at that location. This can be seen at the Pannerdensche Kop. It also increases the bed level difference between the Bovenrijn and the Pannerdensch Kanaal.

The downstream transition zones at the Pannerdensche Kop are very different in the two branches. The downstream transition zone in the Waal is much longer than the upstream transition zone. For the Pannerdensch Kanaal the downstream transition zone is 0 m. This can be linked with the upstream transverse slope and discharge distribution. The bed level at the left side of the Bovenrijn is higher than the equilibrium bed level. The Waal has an opposite curvature compared to the Bovenrijn causing the bed level at the left side of the Waal to be lower than the equilibrium level. This results in a larger bed level difference than only between the two equilibrium levels. This could cause the longer transition zone. This is supported by the identified relationship between difference in water depth and downstream transition zone.

The difference in equilibrium water depth between the Bovenrijn and Pannerdensch Kanaal and the measured difference is very large. This difference can be explained by the transverse slope in the Bovenrijn and the bed level being below equilibrium level at the right side of the Bovenrijn. The non existing downstream transition zone in the Pannerdensch Kanaal can be a result of this as well. The change in bed level in the upstream transition zone could be the change from high transverse bed slope to a flat transverse bed. Since the equilibrium bed levels in the Bovenrijn and Pannerdensch Kanaal are very similar, the change in bed level in a downstream transition zone would be small too; smaller than the present irregularities in the bed level.

### 7.3.2 IJssel Kop

At the IJssel Kop the majority of the discharge flows into the Nederrijn and only one third into the IJssel. The equilibrium water depth is almost twice as deep in the Nederrijn as in the IJssel. However, the measured bed level in the IJssel is lower than that in the Nederrijn. This lower bed level can be due to the change in flow velocity between the Pannerdensch Kanaal and IJssel.

The flow velocity was not part of the bifurcation analysis. However this parameter does impact the way the bed level is shaped. Changes in flow velocity lead to erosion or deposition of sediment. Due to the change in width, depth and discharge ratio up and downstream of the bifurcation, the flow velocity will change. The flow velocity is directly related to the water depth via:  $Q = h * W * v$ . This makes it hard to estimate the flow velocity when the water depth is unknown. This is per definition the case, when the extended rapid assessment tool is applied. Another reason can be that the discharge distribution is often not the assumed two third, one third division, where one third flows into the IJssel. Most of the time the weirs in the Nederrijn are closed. Only when the discharge from the Bovenrijn is above average, the weirs are opened. Till then only  $30m^3/s$  or less flows through the Nederrijn van Deelen and Holleman (2015). Some fine sediment will still flow into the Nederrijn and possible settle there.

### **7.3.3 Danube - Bala bifurcation**

At the end of the transition zone in the Old Danube is a deep pool. The rest of the branch is relatively shallow and has not much variations in depth. This pool might be caused by an error in the measured data. Two data sets have been used to interpolate the bed level onto the grid. At the end of the transition zone in branch 2 is border between those two data sets. This pool at the end of the transition zone has significant consequences for the accuracy of the computed bed level.

### **7.3.4 Other suitable cases**

The extended rapid assessment tool can be applied on other bifurcations. The accuracy of the results will depend on several factors. The most important factor is the accuracy of the physics based model outside the transition zone. When it is possible to calibrate the model, the accuracy will significantly increase. The second factor are the equations to compute the transition zone lengths. These equations will give the best results for bifurcations similar to the scenarios used in the bifurcation analysis. For bifurcations like the Danube - Bala bifurcation, where discharge and river widths are very different, the bed level computed by the extended rapid assessment tool could be less accurate.



# Conclusions, limitations and recommendations

This chapter consists of two sections: firstly, the conclusions drawn from this study and secondly the limitations of the extended rapid assessment tool as well as the recommendations for the application and further research.

## 8.1 Conclusions

The conclusions will be given per research question.

### **Research question 1**

*How does the bed level at a bifurcation look?*

Bed level at bifurcations vary. Influences from outside the transition zone affect the bed level in the transition zone. The transverse slope due to curvature in the river has a bigger influence on the bed level and the transition zone length in the bed level of the Pannerdensche Kop and IJssel Kop than on the bed level of the modelled scenarios. In both the measured data and the modelled data, the bed level becomes more or less flat just upstream of the bifurcation. .

In the Pannerdensche Kop the main flow shifts from the right side of the river to the left downstream branch. The right side of the Bovenrijn is the outer bank of the river. This shift causes the bed level in the transition zone between the right side of the upstream river and the left branch to be deeper than upstream at the left side of the river.

In the Danube are several deep pools just outside of the transition zone. These pools do also shape the bed level in the transition zone. These pools make it seem that the transition zone is longer than it actually is.

The transition from the upstream bed level to downstream bed level is fairly smooth. In the modelled data, bars and pools occurred upstream and downstream of the bifurcation point. In the measured data these are difficult to locate and when they are present, they are not necessarily caused by the bifurcation but can also be other local morphological features.

The groynes in the river have only little effect on the bed level. This effect is negligible compared to the effect of the bifurcation.

### **Research question 2**

*Which physical or empirical relationships describe the bed level at bifurcations?*

Three relationships have been found that describe the length of the transition zone. Two relationships have been identified that describe the length of bars or pools occurring in the transition zone, one also describes the size of them. The relation between river width and upstream transition zone length as described in the literature is confirmed. The other relationship that is found is between river curvature and upstream transition zone length. These two combined gives Eq. 4.1 to describe the upstream transition zone length.

The downstream transition zone is harder to describe. A weak relationship between downstream river width and the downstream transition zone is found. Between difference in water depth and downstream transition zone there appears to be a relationship as well. However, this relationship is deemed unsuitable for implementation in the extended rapid assessment tool. This is because of suspected bias in the observed relationship as well as the limited information available on the difference in water depth due to the scarcity of data.

The bar or pool length is dependent on the length of the transition zone length. Downstream pools or bars have only been analysed for branches where the downstream bed level is lower than the upstream bed level. The size of the pools or bars are depending on the width of the river. However, this parameter seems unlikely to be the determining factor for the size. Other parameters which were not analysed will, most likely, turn out to have a more direct and stronger relation with the bars and pools.

No relationship between discharge distribution and the transition zone length has been identified in this study.

### **Research question 3**

*How can these relationships be implemented in a model?*

The identified relationships can be implemented by assuming that the river is at equilibrium up and downstream of the transition zone. This makes it possible to calculate the bed level there with the physics based model as developed by Zervakis (2015). The bed level in the transition zone can be determined by using various interpolation methods. Three types of interpolation methods have been applied that do not take the bars and pools into account and one that does. Only the linear interpolation method is extended to include bars and pools. This is done by implementing the same schematization as for the bifurcation analysis (Figure 3.2a)

**Research question 4**

*How well does the extended tool perform at approximating the bed level at a river bifurcation*

The performance of the extended rapid assessment tool is very dependent on the performance of the physics based model. The basis for the interpolation in the transition zone is based on the bed level calculated by the physics based model. The four interpolation methods give similar results in all three study cases. Linear interpolation gives the lowest RMSE in two of the three study cases. The addition of bars and pools to the linear interpolation method does increase the accuracy of the extended rapid assessment tool in one study case, in one it is the same as the linear interpolation method and in one case it leads to a higher RMSE.

The RMSE computed when the interpolation in the transition zone is based on measured data shows that linear interpolation gives the highest accuracy. In one case study the linear interpolation method including bars and pools does lead to an increased accuracy, in the other two case studies it does not.

## 8.2 Limitations and recommendations

The major limitation of the approximation of the bed level in transition zones is the accuracy of the bed level data up and downstream of the transition zone. When the accuracy of the up and downstream data is low, all four interpolation methods perform almost equally well.

The upstream transition zone length is now determined by the width and curvature of the upstream river. This is derived from data coming from a model which is based on the Pannerdensche Kop. This means that some of the parameters, that are constant in all scenarios, are typical for the situation around the Pannerdensche Kop. One of these parameters is the discharge, this is kept constant at  $2500 \text{ m}^3/\text{s}$ . Another parameter that is kept constant is the slope of the river. Only in three scenarios, the downstream slope is increased with 10%. These two parameters will have an effect on the flow velocity in the river. This can, in turn, have an effect on the bed level around the bifurcation and both are interesting parameters for further research to further improve the extended rapid assessment tool.

The downstream transition zone length is difficult to determine. The only good indicator that is found is the river width. Because the downstream river width in the modelled data is exactly half of the upstream river width, it cannot be determined if up or downstream river width, or perhaps both, are related to the downstream transition zone length. A study where the downstream river width is varied will give more insight in this aspect. For this study it would be important to not limit the sum of the width of the downstream branches to the width of the upstream river. In all three of the test cases, the upstream width is smaller than the total downstream river width.

The extended rapid assessment tool is one step closer to be able to assess whole river systems. The tool can be useful in situations where a rough estimation of the bed level of a river is required and where the means or time to calculate this are limited. The tool provides

a rough estimation of the bed level around bifurcations. When the bed level generated by the extended rapid assessment tool is used as initial bed level in a 3D morphological model it would probably not significantly increase the accuracy of this model. The difference between a single step approach and linear or Gaussian error function interpolation are too small for this. The added smoothness in the transition from using linear interpolation or Gaussian error function interpolation compared to the single step interpolation, will probably be quickly achieved by the 3D model itself.

To be able to assess full river systems with the extended rapid assessment tool, it will have to be extended at least once more. This in order to take the river convulsions into account too. It is quite possible that the current extended rapid assessment tool is able to approximate the bed level at river convulsions too. However, this has not been tested. The transition zone at a river convulsion can also be very different from the one at a river bifurcation. More research into the bed level at river convulsions and the difference between the bed level at river bifurcations will provide further insight into these aspects.

# Bibliography

- Amsden, A. A. and Hirt, C. (1973). A simple scheme for generating general curvilinear grids. *Journal of computational physics*, 11:348 – 359.
- Andrews, L. (1998). *Special Functions of Mathematics for Engineers*, volume 49 of *Oxford science publications*. SPIE Optical Engineering Press.
- Benson, M. A. and Dalrymple, T. (1984). *Techniques of Water-Resources Investigations of the United States Geological Survey*. USGS.
- Bulle, H. (1926). *Untersuchungen über die Geschiebeableitung bei der Spaltung von Wasserläufen: Modellversuche aus dem Flussbaulaboratorium der Technischen Hochschule zu Karlsruhe*. VDI-Verlag.
- Crosato, A. (2008). *Analysis and modeling of river meandering*. PhD thesis, TU Delft.
- Deltares (2014). *Delft3D - FLOW Simulation of multi-dimensional hydrodynamic flows and transport phenomena, including sediments*. Deltares, Boussinesqweg 1 2629 HV Delft, 3.15.34158 edition.
- Dutta, S., Wang, D., Tassi, P., and Garcia, M. H. (2017). Threedimensional numerical modeling of the bulle effect: the nonlinear distribution of nearbed sediment at fluvial diversions. *Earth Surface Processes and Landforms*, 42(14):2322–2337.
- Engelund, F. and Hansen, E. (1967). A monograph on sediment transport in alluvial streams. *Technical University of Denmark Østervoldgade 10, Copenhagen K*.
- Ernstsen, V. B., Noormets, R., Hebbeln, D., Bartholomä, A., and Flemming, B. W. (2006). Precision of high-resolution multibeam echo sounding coupled with high-accuracy positioning in a shallow water coastal environment. *Geo-Marine Letters*, 26(3):141–149.
- Jantti, T. . (1989). Trials and experimental results of the echos xd multibeam echo sounder. *IEEE Journal of Oceanic Engineering*, 14(4):306–313.
- Kalkwijk, J. P. T. and Vriend, H. J. D. (1980). Computation of the flow in shallow river bends. *Journal of Hydraulic Research*, 18(4):327–342.
- Kenney, J. and Keepings, E. (1962). *Mathematics of Statistics Pt 1*. D van Nostrand, 3rd edition.

- Kleinhans, M. G., Ferguson, R. I., Lane, S. N., and Hardy, R. J. (2013). Splitting rivers at their seams: bifurcations and avulsion. *Earth Surface Processes and Landforms*, 38(1).
- Kleinhans, M. G., Jagers, H. R. A., Mosselman, E., and Sloff, C. J. (2008). Bifurcation dynamics and avulsion duration in meandering rivers by one-dimensional and three-dimensional models. *Water Resources Research*, 44(8).
- Lesser, G., Roelvink, J., van Kester, J., and Stelling, G. (2004). Development and validation of a three-dimensional morphological model. *Coastal Engineering*, 51(8-9):883–915.
- Miori, S., Repetto, R., and Tubino, M. (2006). A onedimensional model of bifurcations in gravel bed channels with erodible banks. *Water Resources Research*, 42(11).
- Papanicolaou, A. N., Elhakeem, M., and Hilldale, R. (2007). Secondary current effects on cohesive river bank erosion. *Water Resources Research*, 43(12).
- Pittaluga, M. B., Repetto, R., and Tubino, M. (2003). Channel bifurcation in braided rivers: Equilibrium configurations and stability. *Water Resources Research*, 39(3).
- Rijkswaterstaat (2018a). Meten bij rijkswaterstaat. Website.
- Rijkswaterstaat (2018b). Waterhuishouding nederland. <https://www.rijkswaterstaat.nl/water/projectenoverzicht/pannerdensch-kanaal-waterhuishouding/waterhuishouding.aspx>. Accessed: 14-06-2018.
- van Deelen, S. and Holleman, C. (2015). Watermanagement en het stuwenssemble nederrijn en lek : voldoende zoetwater, bevaarbare rivieren. Technical report, Rijkswaterstaat.
- van der Veen, R. and van der Veen, S. (2010). Betrekkingslijnen Rijn. Technical report, RURA-ARNHEM.
- Wang, Z., Fokking, R., de Vries, M., and Langerak, A. (1995). Stability of river bifurcations in 1d morphodynamic models stabilite des bifurcations de rivieres dans des modeles morphodynamiques filaires. *Journal of Hydraulic Research*, 33(06):739–750.
- Wood, J. and Fisher, P. (1993). Assessing interpolation accuracy in elevation models. *IEEE Computer Graphics and Applications*, 13(2):48–56.
- Yossef, M. F. M. (2013). Progress report ii - data report. Technical report, Deltares.
- Zervakis, D. I. (2015). Combining a physics-based model and spatial interpolation of scarce bed topography data in meandering alluvial rivers. Master's thesis, Delft University of Technology.
- Zinger, J. A., Rhoads, B. L., Best, J. L., and Johnson, K. K. (2013). Flow structure and channel morphodynamics of meander bend chute cutoffs: A case study of the wabash river, usa. *Journal of Geophysical Research: Earth Surface*, 118(4).

# Scenarios in Kleinhans et al. (2008)

The standard scenario for the runs consists of a grid of 80 cells long and 20 wide. The cells are 150 m long and 28 m wide. The bifurcation is located in the middle of the grid. At the bifurcation two rows of cells are lost, this is compensated by increasing the width of the downstream cells in such a way that the total width downstream and upstream is equal. This increase in width of the cells takes place in the first 5 cells downstream of the bifurcation. The radius of the bend of the downstream branches is equal to 20 times the width of the branch. The radius of the bend of the upstream branch is varied in the scenarios. The first 17 cells upstream of the bifurcation are bend the other 23 cells are straight. The discharge is  $2500 \text{ m}^3/\text{s}$  and the roughness is 0.15 m, using the Darcy-Weissbach equation. The initial depth is 3 m and the slope is 0.1 m/km. The morphological factor was 100 and the time period of one run is 263000 minutes with a time step of 0.5 minutes.

In scenarios 1 - 7 is the radius of the bend of the upstream branch varied. In Table A.1 are the factors shown that determine the bend radius. The width of the upstream branch is multiplied by this factor to get the bend radius.

In scenario 8, 9 and 10 are the width of the cells varied, see Table A.2.

In scenario 11, 12 and 13 is the slope of the downstream inner branch is steeper and the radius of the upstream bend is varied. The slope and bend radius factor per scenario is shown in Table A.3.

Scenario	Bend radius factor
1	100
2	50
3	20
4	10
5	8
6	6
7	4

**Table A.1:** Scenarios with varied bend radius

Scenario	Cell Width [m]	Total width [m]
8	35	700
9	21	420
10	16	320

**Table A.2:** Scenarios with varied cell width

Scenario	Slope [m/km]	Bend radius factor
11	0.11	100
12	0.11	10
13	0.11	4

**Table A.3:** Scenarios with steeper slope

# Method to create a grid around bifurcations

The grid is created in 4 steps. These will be explained here in separate sections. The input for the creation of the grid are the points that describe the surface of the river at the bifurcation. The input consists of the coordinates of the river banks, three points in every branch and the amount of horizontal and vertical lines in the grid.

## **B.1 Finding bifurcation point**

The first step is to find the point where the grid will bifurcate. This is done by creating a Voronoi tessellation in the polygon. This Voronoi tessellation is cleaned up, all points that are not in the centre line of the river are removed. The remaining points are used to find the bifurcation point. This is done by comparing the angle of three points. If this angle is larger than the threshold it means they are not one a line and thus at a bifurcation point.

## **B.2 Preparation**

The horizontal spacing of the grid is based on the distance between the distance between the given point in branch 0 and the point derived from the mean of the two points in the two branches. The vertical spacing is based on the width of the river at the start. The grid is positioned at the same angle as the upstream river.

## **B.3 Moving vertices**

The corner vertices of the grid are moved to the desired location. This at both banks of the river near the three points that specify the location of the three branches. Next the borders of the grid are moved, until they are aligned with the border of the given polygon. The vertices in the middle of the grid move until they are evenly spaced between the river banks.



# Groynes analysis

In Figure C.1 are the location of the groynes shown and the bed level of the river. There are some local banks or ripples in the bed level. However, location the peaks or troughs seem to have no relation to the location of groynes. Sometimes groynes are located at a trough, sometimes at the peak or somewhere in between. The banks or ripples in the bed level are of a much smaller scale than the changes in bed level caused by the bifurcation.

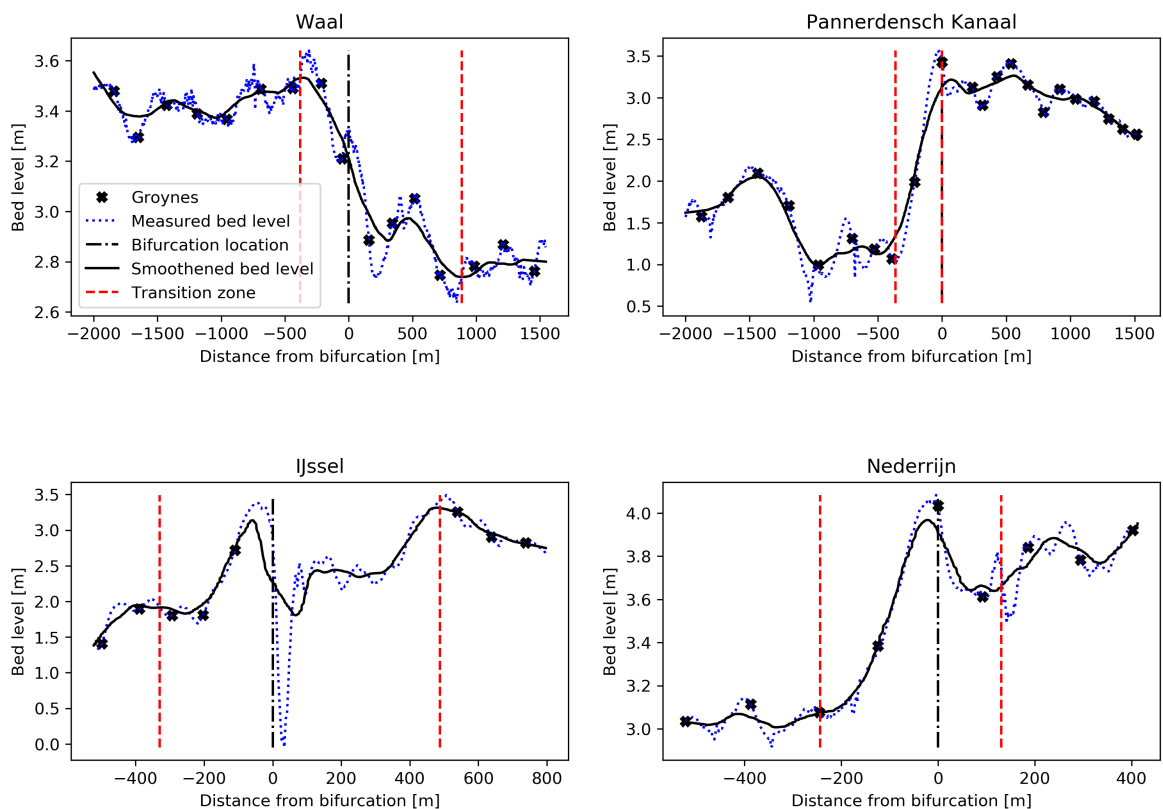


**Figure C.1:** Location of the groynes in the branches around the Pannerdensche Kop and IJssel Kop.



# Study case results

## D.1 Pannerdensche Kop

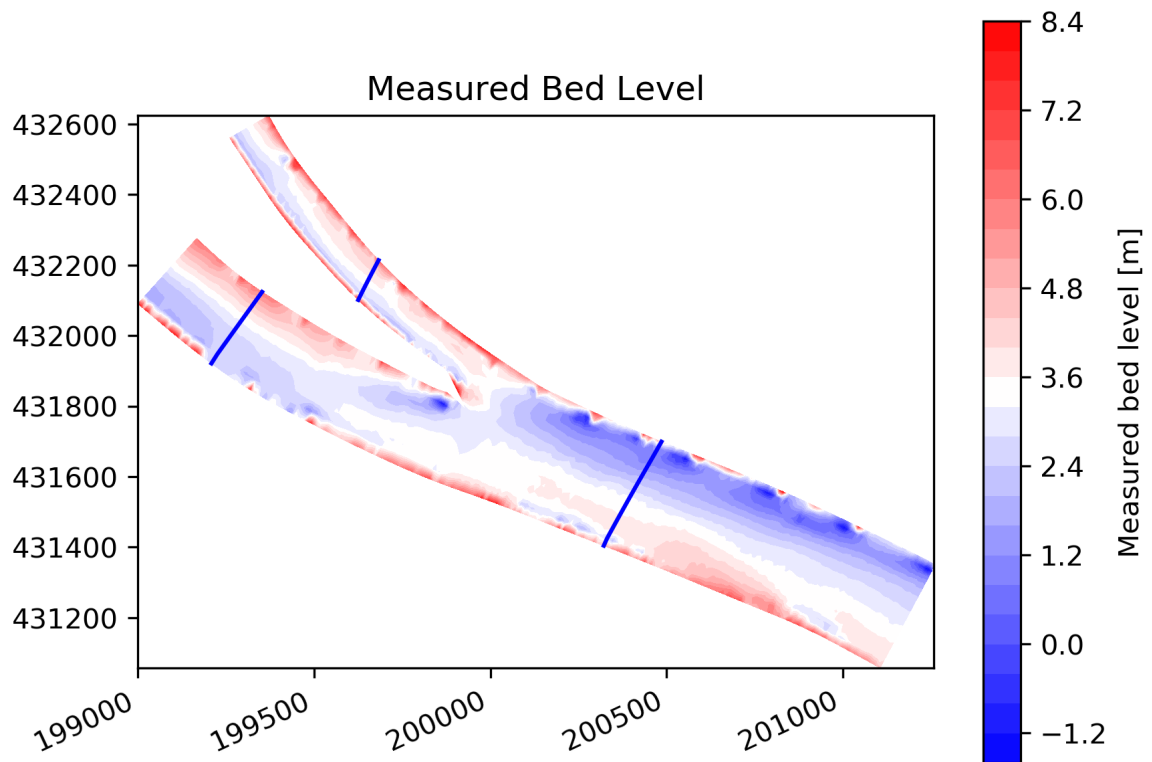


**Figure D.1:** The measured bed level around the Pannerdensche Kop

For all following figures: (a) The error map and (b) the modelled bed level, based on the physics based model. (c) The error map and (d) the modelled bed level, based on measured data. The blue lines indicate the begin and end of the transition zone

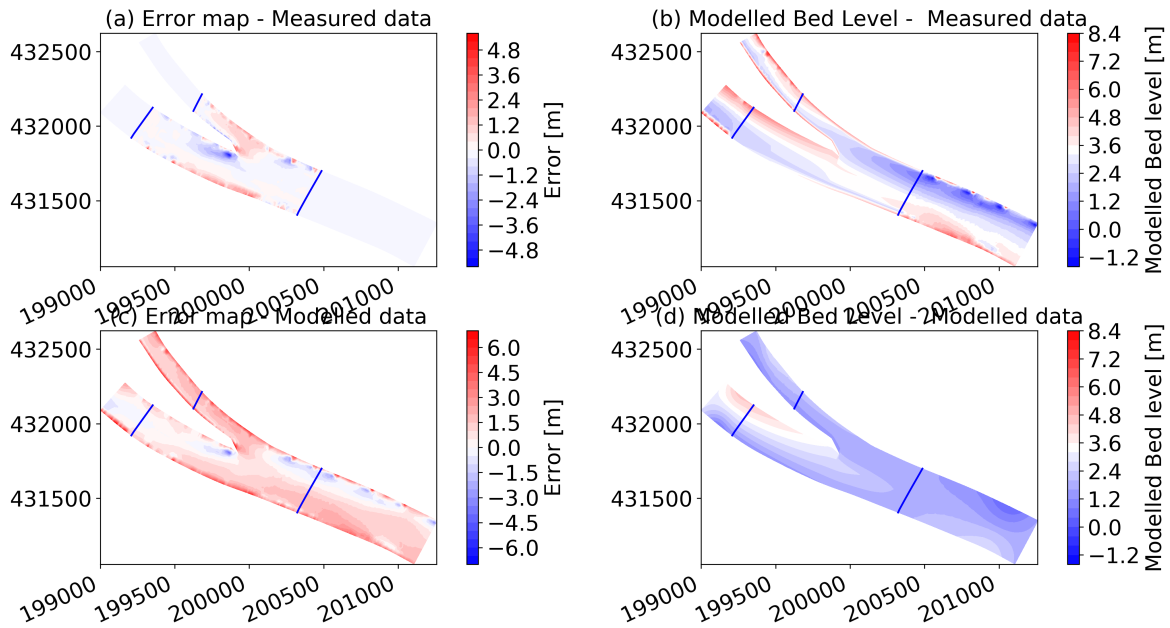


**Figure D.2:** Pannerdensche Kop - Linear interpolation method

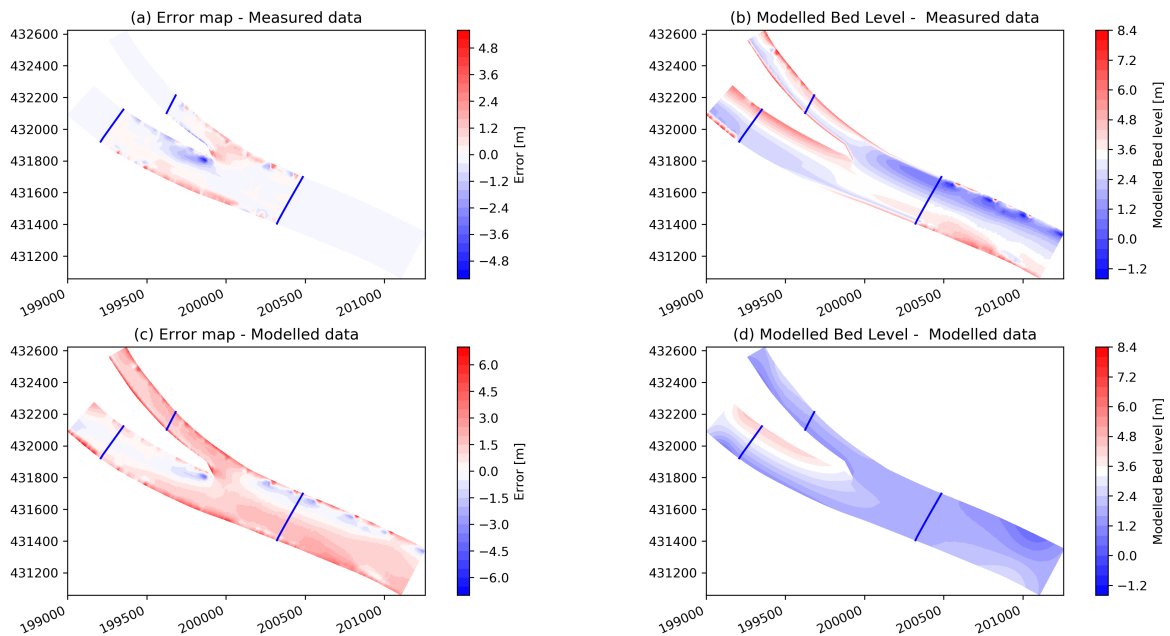


**Figure D.3:** Pannerdensche Kop - Gaussian error function interpolation method

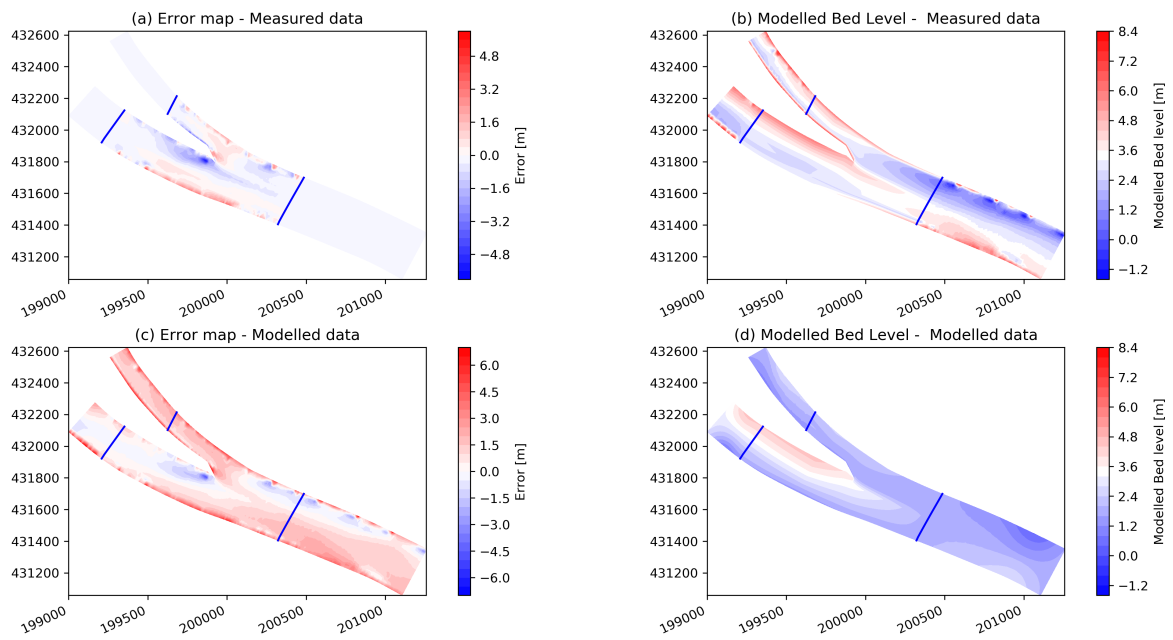


**Figure D.4:** Pannerdensche Kop - Linear interpolation including bars and pools method

## D.2 IJssel Kop

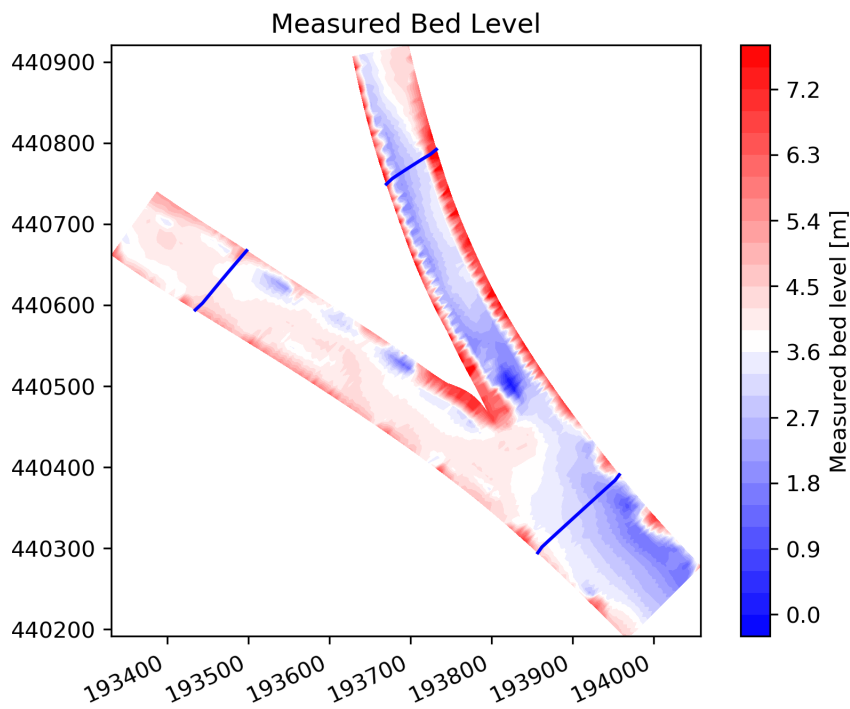


Figure D.5: The measured bed level around the IJssel Kop

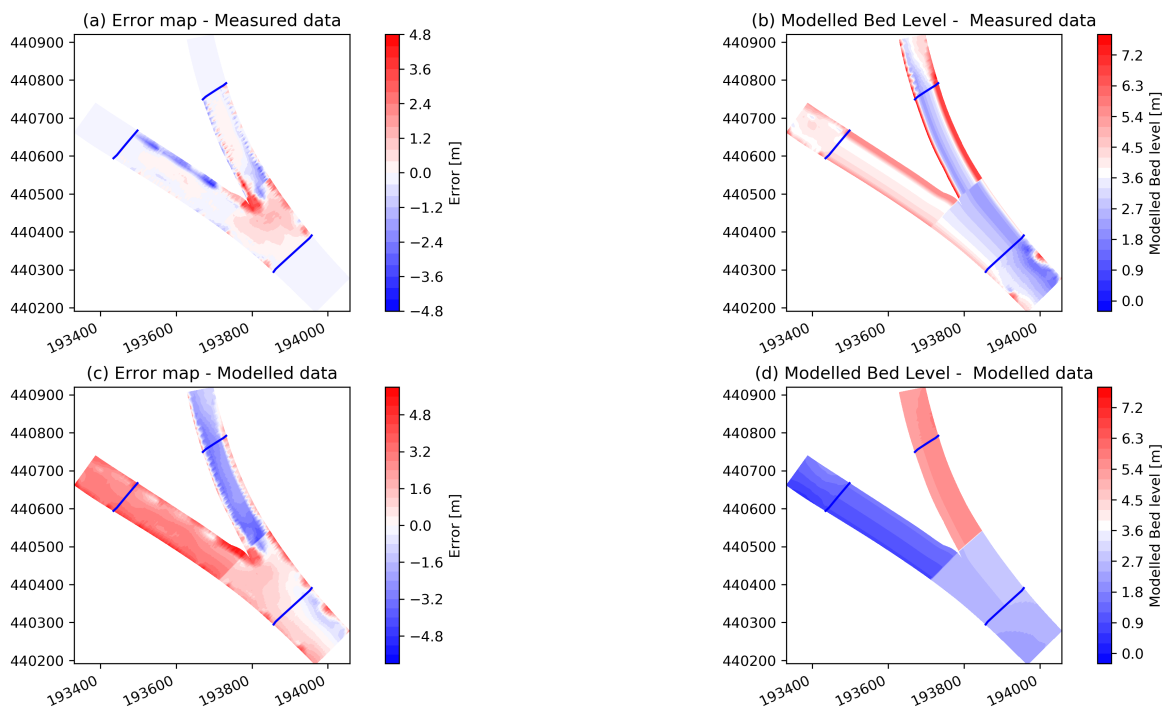


Figure D.6: IJssel Kop - Single step interpolation method

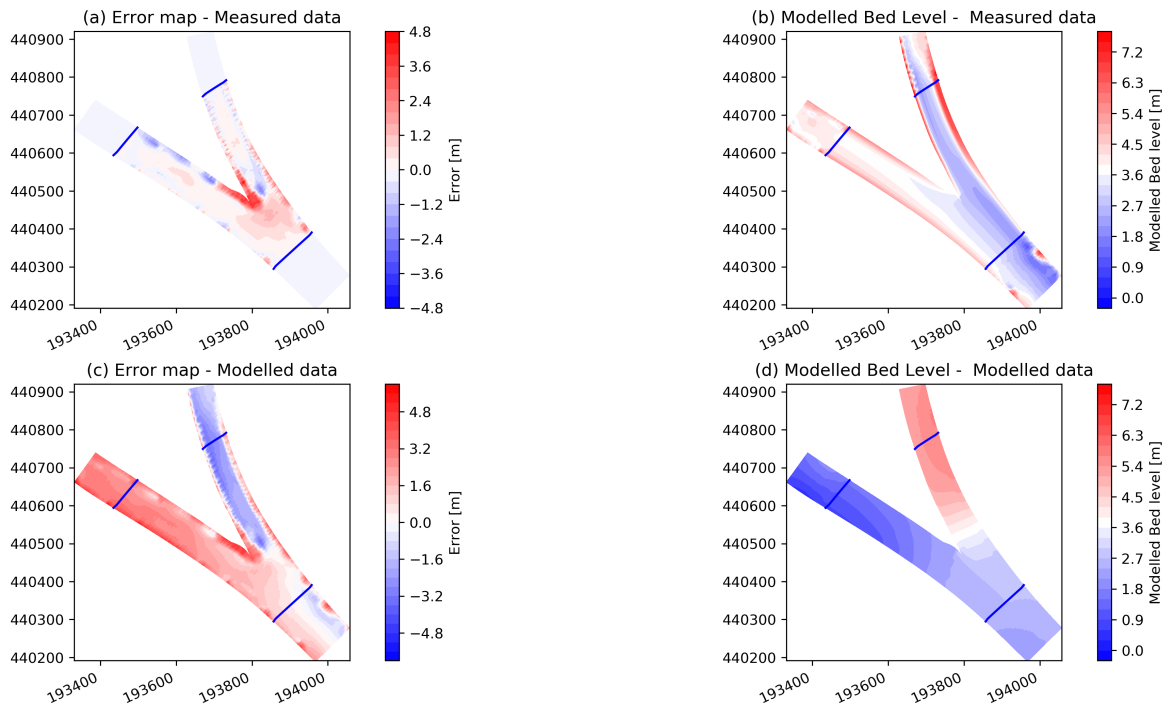


Figure D.7: IJssel Kop - Gaussian error function interpolation method

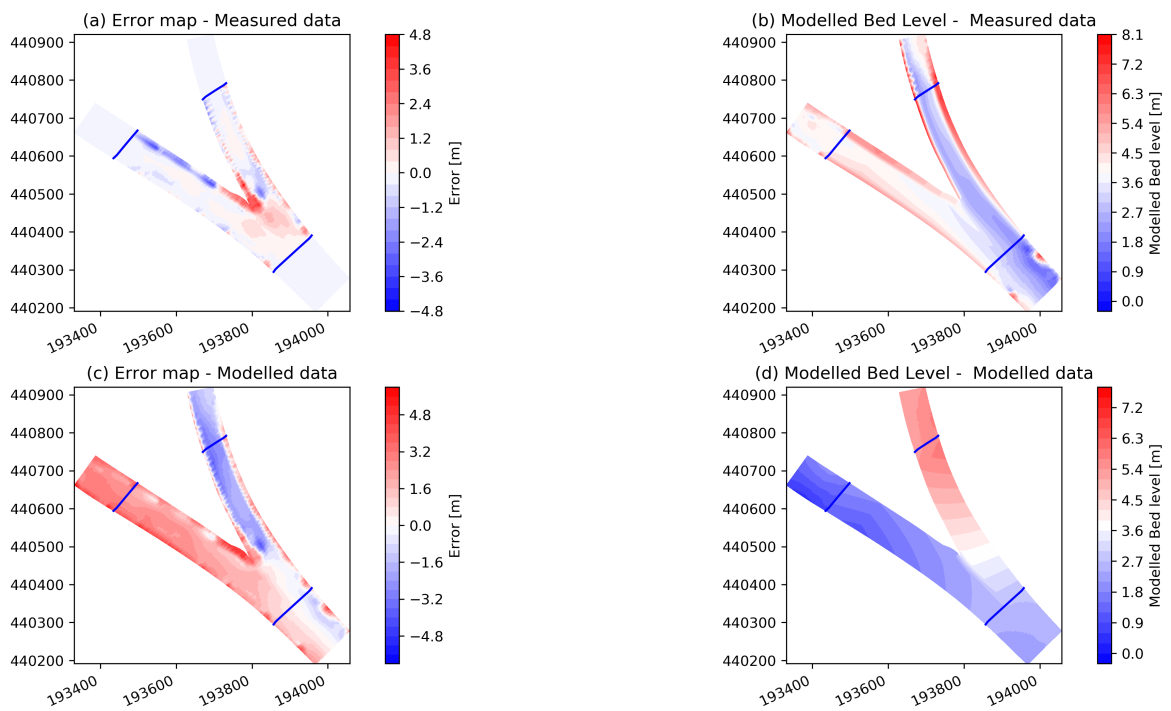
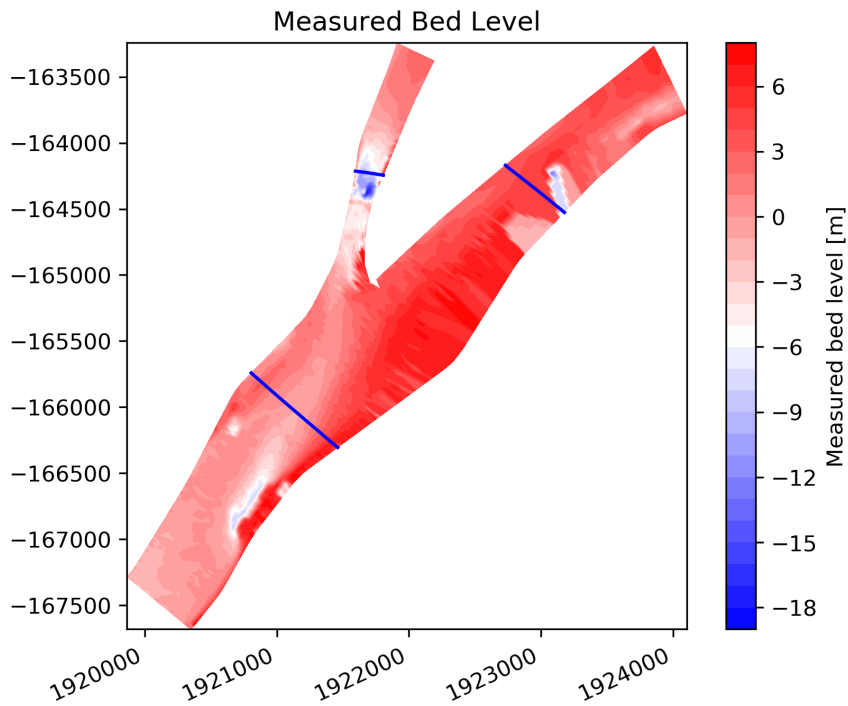
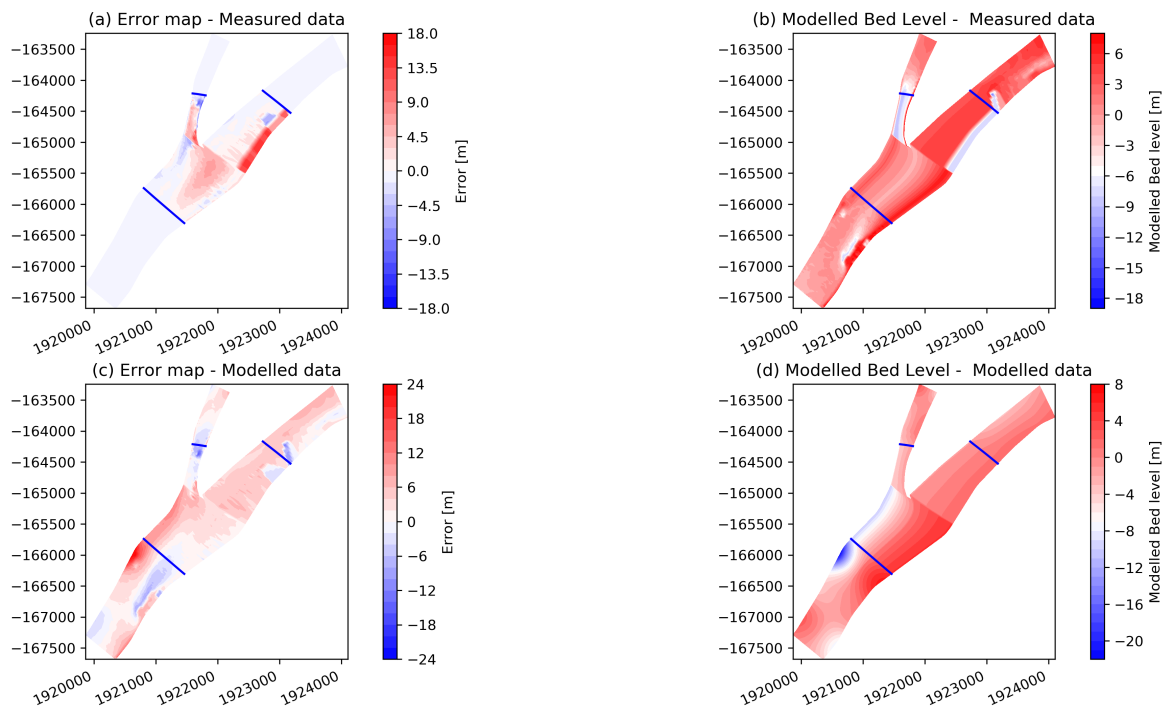


Figure D.8: IJssel Kop - Linear interpolation including bars and pools method

### D.3 Danube - Bala bifurcation



**Figure D.9:** The measured bed level around the Danube - Bala bifurcation



**Figure D.10:** Danube - Bala - Single step interpolation method

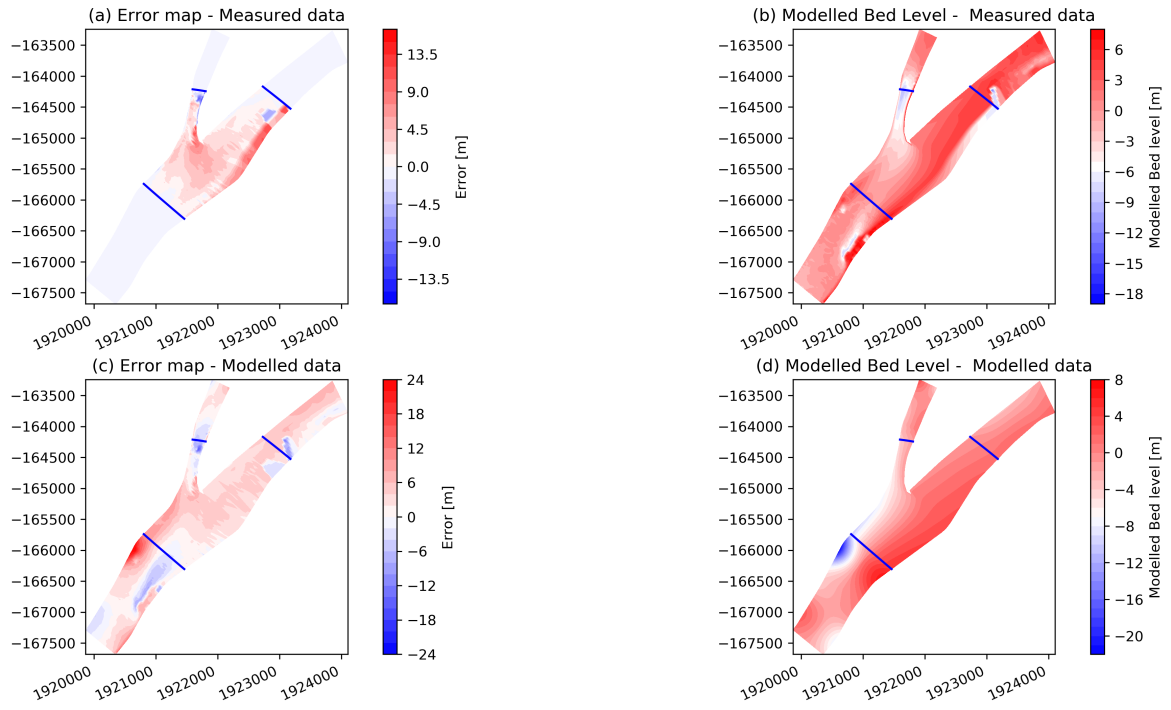


Figure D.11: Danube - Bala - Linear interpolation method

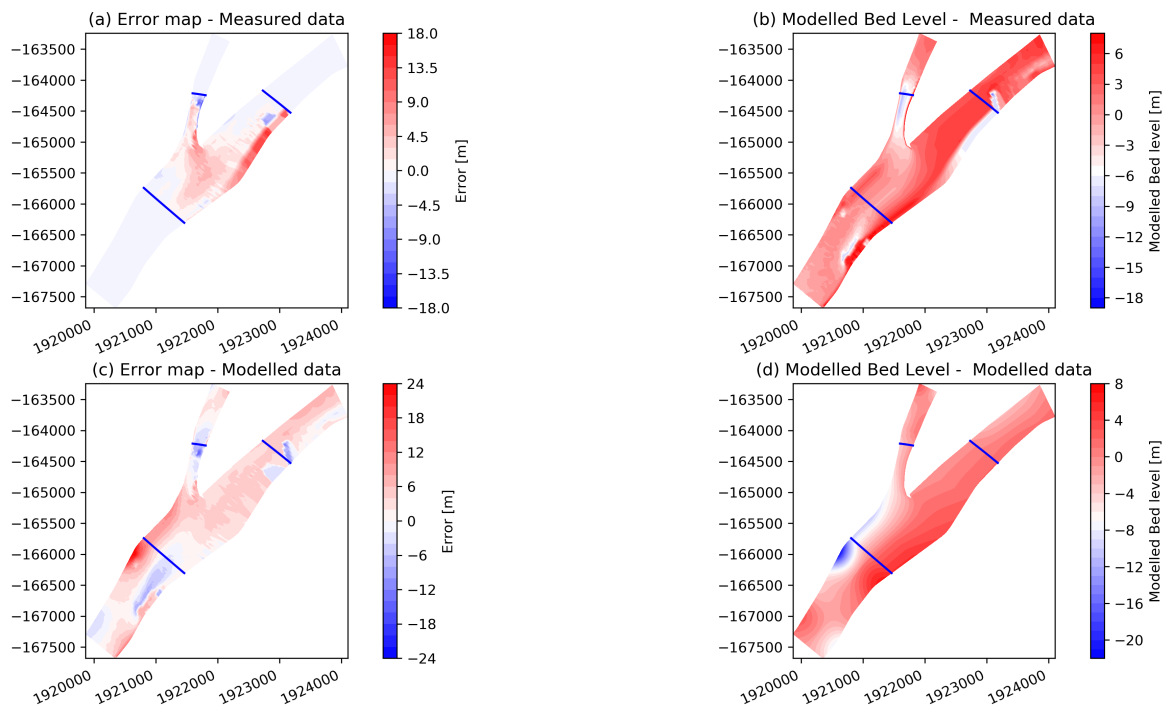


Figure D.12: Danube - Bala - Linear interpolation including bars and pools method